MINISTRY OF EDUCATION
NATIONAL UNIVERSITY OF SCIENCE AND TECHNOLOGY POLITEHNICA BUCHAREST
FACULTY OF POWER ENGINEERING
Splaiul Independenţei 313, Sector 6, 060042 Bucharest, Romania
Tel: +40 21 402 9433; Fax: +40 21 318 1015; http://www.energ.upb.ro/

NATIONAL UNIVERSITY OF SCIENCE AND TECHNOLOGY POLITEHNICA BUCHAREST

Class of
July 2024

Faculty of Power Engineering
Department of Hydraulics, Hydraulic Machinery and Environmental Engineering
Bachelor's programme: *Hydropower Engineering*

Floating Photovoltaic Panels: Assessing the Potential, Advantages and Challenges of Harvesting Solar Energy on Water Surfaces

Bachelor's Student
Aurelian-Andrei Panait

Scientific Coordinator
Assoc. Prof. Dr. Eng. Liana Ioana VUŢĂ

MINISTRY OF EDUCATION
NATIONAL UNIVERSITY OF SCIENCE AND TECHNOLOGY POLITEHNICA BUCHAREST
FACULTY OF POWER ENGINEERING
Splaiul Independenţei 313, Sector 6, 060042 Bucharest, Romania
Tel: +40 21 402 9433; Fax: +40 21 318 1015; http://www.energ.upb.ro/

Floating photovoltaic panels: harvesting solar energy on water surfaces

Abstract

The worldwide transition to a net-zero-emission future depends to a large extent on solar energy. However, as land prices rise and population density increases, the need for large land areas for the development of solar farms poses significant difficulties. Floating Photovoltaics (FPV) have emerged as a viable solution to this problem. FPV, which involves mounting solar panels on water surfaces, is gaining popularity as a practical solution around the world. A significant capacity of 404 GWp of green energy generation could be achieved by using FPV to cover only 1% of the world's reservoirs. In what follows, we show that FPV offers several advantages over ground-mounted photovoltaic systems. On the other hand, few studies address the effects of FPV on water quality and aquatic ecosystems. This analysis examines the most recent FPV research, including its advantages, disadvantages and potential. The compatibility of different water bodies, the worldwide potential, system efficiency and the possibility of integrating various technologies with FPV are investigated.

Keywords: floating photovoltaic panels, solar energy, water surfaces, solar potential assessment, geospatial techniques.

CONTENTS

LIST OF FIGURES

LIST OF TABLES

LIST OF ABBREVIATIONS

FPV Floating Photovoltaics

GHI Global Horizontal Irradiance

DNI Direct Normal Irradiance

GPV Ground-mounted Photovoltaics

NRL Normal Retention Level

a.s.l. above sea level

INTRODUCTION

The need for energy grows together with the global population, leading to the use of more fossil fuels that produce greenhouse gases [6]. The world is searching for strategies to minimise greenhouse gas emissions as climate change worsens [13]. According to the International Energy Agency (IEA), average annual solar energy production must increase by 24% for the world to reach net-zero emissions by 2050 [37].

Future energy sources are anticipated to include photovoltaics (PV). At present, PV costs are roughly on par with those of traditional energy sources, owing to a steep decline in PV prices [43]. According to the IEA, PV has historically been the cheapest source of electricity [59]. Although the installed PV capacity is expected to grow, ground-mounted photovoltaic (GPV) farms struggle to find land for installation [17]. Approximately 15,000 m^2 of land are required for a 1 MW PV farm [17]. It is becoming increasingly difficult to find land for building a PV farm because of the enormous land requirements and rising land prices. PV installations must also contend with issues such as cooling and keeping the panels free of dust in order to increase efficiency and energy yield [33]. Placing PV panels on water surfaces, such as wastewater treatment facilities, oceans, lakes, lagoons, canals, ponds, reservoirs or irrigation basins, is one way of solving the problem of land-use regulations for solar energy projects. This technique allows water surfaces to be used for solar energy generation, potentially resolving the shortage of available land and the high cost of land.

Floating photovoltaic (FPV) systems can help increase solar energy capacity while reducing the need for substantial land resources by making use of available water surfaces [35]. This research on FPV explores solar energy generation and its integration on water surfaces. It focuses on the optimisation of energy systems, building on a previous study on energy storage systems and their impact on grid peak-load shaving [40]. That study aimed to determine the optimal placement and capacity of energy storage and to establish a charge–discharge strategy for such systems. Genetic Algorithm (GA) and Particle Swarm Optimisation techniques were used to compute the minimum and maximum loads in the grid, taking energy storage systems into account.

The present analysis aims to assess the current state of FPV, together with its advantages and disadvantages. The first FPV plant was established in Japan in 2007 [61], making it a relatively young technology. The installed PV capacity is currently doubling every year and is expected to continue at the same pace [10].

At present, FPV is more expensive than GPV, with a 4–8% increase in design costs [17]; this makes the present assessment important and timely, since the industry is experiencing significant global growth but there is still little understanding of the potentially harmful effects of FPV.

CHAPTER 1
TECHNOLOGY OVERVIEW

The installation of solar panels on water relies on floating platforms, which offer potential advantages over conventional land-based installations. In recent years, interest in this innovative strategy has grown [7]. Figure 1.1 illustrates a standard FPV system composed of PV panels and a floating structure securely anchored to the ground.

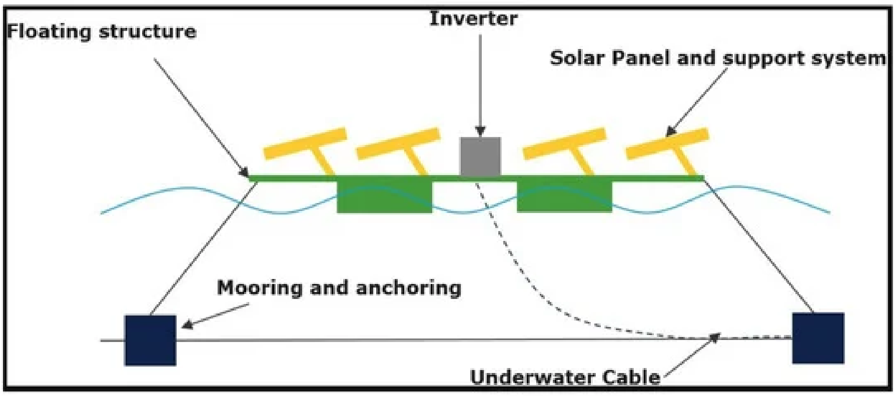

Fig. 1.1: FPV structure

1.1 Floating Photovoltaic Systems

1.1.1 Floating platforms

A pontoon construction keeps the apparatus afloat on the water [15], with floats connected together to form pontoons that support the weight of the structure above the water [28]. High-density polyethylene (HDPE), which is maintenance-free, UV-resistant, recyclable, corrosion-resistant and has excellent tensile strength, is used to manufacture most of the floats used in the industry [46]. Glass-fibre-reinforced plastic is another, although less common, material used for floats [3]. These systems usually have fixed panel tilt angles that are difficult to change after installation. Floating structures have the advantage of being easier to dismantle than a GPV system [55]. Additional possibilities for floating structures include one- or two-axis tracking platforms and galvanised steel supports [9]. There are numerous types of floating platforms available for FPV systems, which can be divided into the following categories:

1.1.2 Buoyancy-based platforms

The most popular FPV platform consists of several floating modules joined together to create a stable floating platform. Buoyancy-based platforms are often affordable, modular, and easy to install and disassemble [58]; however, they are less stable in rough waters and, because of their low freeboard height, flooding is more likely.

1.1.3 Semi-submersible platforms

These platforms can be partially submerged in water, increasing stability and reducing the risk of flooding [36], as shown in Figure 1.2. Semi-submersible platforms cost more than buoyancy-based ones and, in addition, involve complex installation and maintenance requirements.

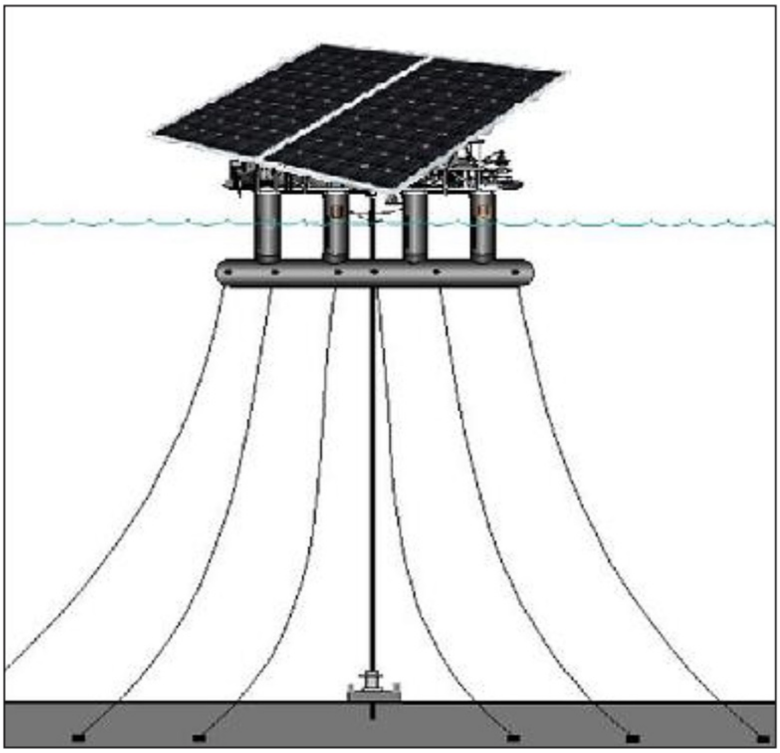

Fig. 1.2: Design of semi-submersible platforms

1.1.4 Tension-leg platforms

Tension-leg platforms allow for larger FPV systems and are highly stable because they are anchored to the seabed using tensioned cables [56], as shown in Figure 1.3. They are more difficult and more expensive to deploy and maintain than other types of platforms.

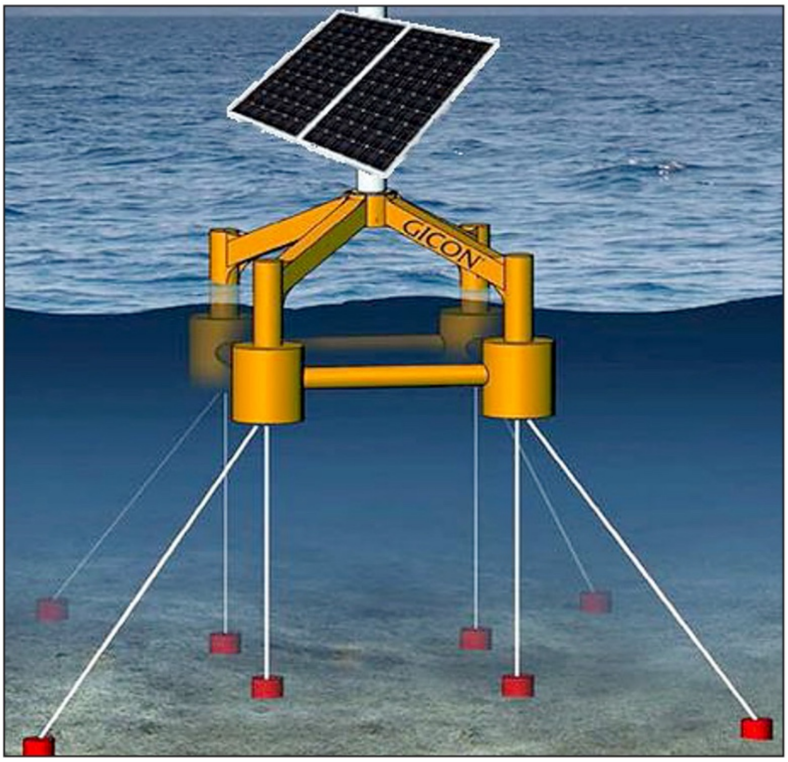

Fig. 1.3: General view of a tension-leg platform

1.1.5 Floating pontoons

Solar panels installed on a series of pontoons anchored to the ocean floor make up floating rafts [53], as shown in Figure 1.4. They are easy to install and maintain, but can be prone to capsizing in rough waters because of the way wave conditions affect their stability.

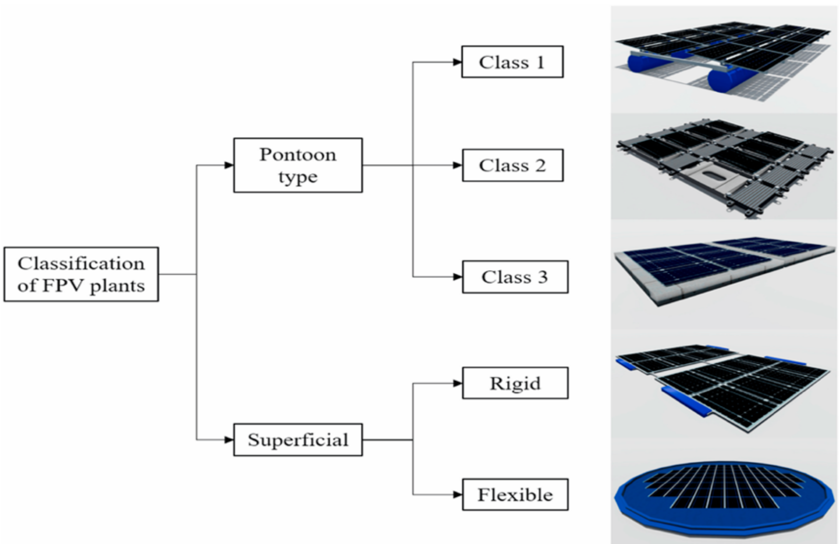

Fig. 1.4: Floating pontoons with installed solar panels

1.2 Photovoltaic Panel Modules

Crystalline silicon is the most frequently used module type in FPV systems [39]. Crystalline modules perform well in freshwater environments, but as the industry turns its attention towards marine environments, the modules must be built to withstand saline conditions. Consequently, an alternative material will have to be used instead of the traditional metal frames. Indeed, second-generation solar technologies such as cadmium telluride (CdTe), amorphous silicon (a-Si) and copper indium gallium selenide (CIGS) are practical options for FPV systems.

1.2.1 Second-generation CdTe

A thin layer of cadmium telluride serves as the light-absorbing layer in CdTe solar panels. CdTe panels are popular for large-scale installations owing to their high conversion efficiency and low manufacturing costs. In addition, CdTe panels are also less sensitive to high temperatures and low light levels compared with certain other technologies [30].

1.2.2 Amorphous silicon (a-Si)

Non-crystalline silicon is used to create a-Si solar panels, allowing for flexibility and a lightweight design. a-Si panels perform better in diffuse-light conditions, such as on cloudy days or in shaded regions, despite their lower conversion efficiencies compared with other technologies. Owing to the reflections and ripples on the water surface, this characteristic can make them useful for FPV applications where light conditions may vary [41].

1.2.3 Copper indium gallium selenide

CIGS solar panels are composed of thin films of copper, selenium, gallium and indium; they perform well in low-light situations and have excellent conversion efficiencies. Owing to their flexibility, CIGS panels can adapt to curved or uneven surfaces. This flexibility can be useful for FPV installations that may need to adapt to the curvature of the water surface [62].

At present, third-generation PV technologies are not used for FPV systems because of their relatively early stage of development and deployment [29].

1.3 Mooring Systems

A mooring system is required to prevent FPV systems from capsizing or drifting. The apparatus is firmly attached to the ground or seabed using anchors [47]. Mooring lines are usually made of nylon ropes, allowing the system to adjust to changes in wind and water depth. Depending on the project budget, water depth, seabed conditions and other parameters, the anchoring method may be gravity-based, drag-embedded, suction-based or tension-based. It is essential to consider the long-term performance and reliability of the mooring mechanism in order to ensure the safety and stability of the FPV platform in challenging marine environments.

1.4 Cables

Cables are essential to the operation of FPV systems, as they connect the solar panels to the power inverter located on the platform. Underwater cables transmit the system's electricity and can carry the energy to an onshore substation [34]; in addition, wires are frequently raised above the water surface. Cables must be carefully engineered when used in FPV systems in order to withstand the harsh marine environment, which includes exposure to salt water, waves and wind.

Finally, the cables installed for FPV systems must be able to adjust to varying water levels and wind in order to move the platforms and send data to monitoring stations. Aluminium, copper or a mixture of these materials is used.

1.5 Electrical Safety

Electrical safety standards are essential for achieving reliable, safe and secure FPV systems, especially since electric shock and corrosion can be avoided through adequate earthing, insulation and training. The FPV electrical system is protected from overloads and hazards by installing safety devices such as surge protectors and circuit breakers. Worker safety is guaranteed through lockout/tagout procedures, adequate training and personal protective equipment (PPE). In addition, regular maintenance, such as component replacement and corrosion testing, ensures the integrity of the system [34].

During the design process, electrical safety factors such as component placement, cable management and earthing requirements must be taken into account. FPV systems can operate safely and productively by complying with all relevant laws and regulations.

1.6 Installation and Location

As long as the mooring and towing mechanism is not excessively complex, installing FPV systems is often easier than installing GPV systems [57].

FPV systems are usually assembled on land before being transferred onto the water, where they can simply be towed to the desired installation area without the need for complicated machinery.

Several factors must be considered when choosing a location for an FPV installation. Table 1.1 lists the key factors that must be evaluated before deciding on an FPV site. Weather, location, terrain and water conditions, among others, can all affect an FPV system. The location of the system is crucial, since solar irradiation levels fluctuate depending on the latitude and longitude of the site. Solar radiation levels are higher in regions close to the equator than in those close to the poles. The effectiveness of the mooring system in ensuring stability and safety in challenging marine situations can be affected by soil and water conditions. The chosen floating platform style must be suitable for the water in which it will be installed. In addition, weather elements such as clouds, rain and fog can affect the amount of solar irradiation, influencing the performance of the FPV system.

Table 1.1: Site selection (Solar Energy Research Institute of Singapore, 2018)

Conditions	**Criteria**
Water characteristics	Limited wave activity Fresh water with low hardness Low salinity
Soil characteristics	Compact soil suitable for anchoring Consistent terrain
Location	No shading caused by landforms and/or neighbouring structures Convenient transport Proximity to the electrical connection Easy installation and maintenance
Weather	Low occurrence of rain and fog Abundant sunlight Wind speeds not exceeding 30 m/s

1.7 Performance and Efficiency of Floating Photovoltaic Panels

1.7.1 The effect of temperature

High temperatures adversely affect the performance, energy production, efficiency and lifetime of PV modules, since high temperatures convert sunlight into heat instead of electricity, making module temperature the most significant factor affecting efficiency [26]. To mitigate the impact of high temperatures on PV modules, various cooling techniques have been explored [14].

An effective approach involves the use of FPV systems, which take advantage of placing PV modules on water surfaces in order to benefit from the cooling effect. This cooling effect improves module efficiency, resulting in higher annual energy production. Studies have indicated that this cooling effect can lead to an efficiency increase of 1.5% to 12.5% for FPV systems compared with GPV systems, depending on the specific climatic conditions of the site. The cooling effect, facilitated by the circulation of cool air beneath the PV modules, is a significant advantage of FPV systems over GPV systems [42].

1.7.2 Humidity

An increase in module humidity is another consequence of placement near water. Compared with GPV modules, FPV modules endure increased humidity. The performance of a module can be negatively affected by an increase in ambient humidity [31].

FPV systems can be affected by humidity in several ways:

- **Reduced efficiency:** high humidity levels can affect the efficiency of PV panels by increasing the cell temperature, which can lower the output voltage and current. As a result, the power output of solar cells decreases as temperature rises.
- **Corrosion:** since FPV systems are frequently installed in humid areas, such as those close to the water surface, exposure to excessive humidity can shorten the lifetime of the metal components of PV panels.

- **Condensation:** excessive humidity can lead to condensation on the surfaces of PV panels, reducing the amount of sunlight reaching the cells, which leads to lower generated output power.
- **Salt deposition:** in coastal regions, high humidity levels combined with salt-laden air can cause salt to accumulate on PV panel surfaces, lowering their efficiency over time.

Designing and installing corrosion- and humidity-resistant FPV systems is crucial [11], as is the regular cleaning of the panels to remove any salt build-up or other impurities that could reduce their performance.

1.7.3 Water evaporation

One of the economic benefits of using FPV is its capacity to mitigate water evaporation from water bodies such as reservoirs [20]. By creating shade, the solar panels reduce the amount of sunlight reaching the water, thereby diminishing the amount of water that evaporates and improving water quality. This becomes crucial for areas facing a water crisis. It has been determined that FPV installation had a significant positive impact in the water-scarce regions of Central and South Asia [4]. In India, the state of Maharashtra installed a 1 MW FPV system on the Ujjani reservoir, generating 1.6 million units of electricity annually and reducing water evaporation by 1.3 million cubic metres per year, resulting in estimated cost savings of 30 million INR (approximately 400,000 USD). Another study examined the environmental impact, economic viability, electricity production and water-evaporation reduction achieved by deploying FPV on the five largest reservoir lakes in Iran. By implementing FPV systems on 10% of the five large reservoirs, it is possible to save a significant amount of water from evaporation. FPV systems can significantly reduce water evaporation, benefiting Iran given its current water and energy crises. This can satisfy the domestic water requirements of approximately one million people, reducing water evaporation and salinity and improving water quality. Studies show that FPV systems can reduce water evaporation by up to 70% [21]. By conserving water resources and improving water quality, FPV systems can help meet the increased demand for water while reducing the environmental impact of energy production.

1.7.4 Impact on water quality

Owing to the lack of available information, the rapid growth of the FPV industry has raised concerns about how it might affect water quality. The greatest danger posed by FPV systems is the potential impact they may have on water quality. Despite FPV operators' claims of low impact on water quality, the study conducted in [19] indicated that only 15% of them actively monitor and analyse water quality, with the majority relying exclusively on visual examination [18]. The impact of FPV installations on nine ecological services was also investigated in that study. In another study, which carried out an experiment using two neighbouring agricultural ponds, one equipped with FPV and the other left uncovered as a control, no harmful effects on water quality due to the presence of FPV were observed. However, the study by Abdelal Q. [2] reported elevated levels of nitrates and chlorophyll, together with a significant 60% reduction in water evaporation. Various research studies indicate that FPV systems can contribute to reducing algae growth and improving water quality [5]. The extent to which FPV affects algae growth depends on the water-surface coverage. Research on the impact of FPV on water quality suggests that a small coverage area of a reservoir with FPV may not be sufficient to prevent algal blooms [27].

An important concern raised in a study examining the impact of FPV on water quality is the limited number of comprehensive studies and models available to correctly identify any potential negative effects.

1.8 Reduction and Protection of Agricultural Land

Countries with high population density encounter difficulties in locating suitable land for PV solar farms, resulting in potential conflicts with other land users and environmental damage such as soil erosion and habitat destruction [22].

FPV offers a solution to this problem by allowing solar panels to be installed on water surfaces that would otherwise be underutilised. FPV systems offer the flexibility of being installed on various water surfaces, such as lakes, ponds, canals, reservoirs, lagoons, wastewater treatment facilities, irrigation ponds and even in small island communities that have limited available land space [8]. Especially in urban areas where land is scarce and expensive, FPV systems can help mitigate land-use conflicts and reduce the demand for land by using water resources for solar energy generation. Compared with GPV systems, FPV installations often involve lower costs, since land does not need to be purchased and land approvals are not required [23]. A techno-economic study conducted in Islamabad exemplified this advantage: a GPV system had a payback period exceeding 15 years, whereas a floating system installed on NUST Lake, an urban lake, had a significantly shorter payback period of 5.37 years.

FPV can help preserve agricultural land, which is essential for food production. FPV can contribute to sustainable land management and food security by reducing the use of agricultural land for solar energy production [45].

1.8.1 Minimising the damage caused by solar energy generation to ecosystems and natural habitats

FPV can reduce the damage caused by solar energy generation to ecosystems and natural areas. Water quality, wildlife habitats and soil condition can all be negatively affected by land-based PV solar installations. The impact of FPV systems on water bodies and aquatic species, on the other hand, can be reduced through careful design and installation [18].

Finally, the use of water bodies for FPV has additional advantages, including reduced water evaporation and improvements in water quality and algal-bloom control, which can be particularly important in dry and semi-arid areas with limited water resources.

In short, reduced land use is a significant economic and environmental factor for FPV: it can reduce land-use conflicts, protect agricultural land, reduce the impact on natural habitats and provide additional environmental benefits by using water surfaces for solar energy generation.

1.8.2 Shading and soiling

Owing to the positioning of FPV on flat surfaces, FPV rarely experiences performance problems caused by nearby shading [48]. A significant issue that lowers the energy production of a PV system corresponds to soiling losses caused by the accumulation of dust deposited on PV systems. In addition to providing renewable energy, FPV can also offer shade for aquatic plants and fish, creating a more favourable environment for aquaculture operations. For example, in the Netherlands, a 2 MW FPV system was installed on a lake, supplying electricity to a nearby dairy farm and creating a shaded area for fish farming [61].

Soiling losses, which reduced electricity generation by 3% to 4% in 2018, resulted in a revenue loss of 3–5 billion EUR [16]. Soiling losses are expected to cause a revenue loss of 4–7 billion EUR by 2023. By 2040, 7200 TWh of solar energy will be produced globally, making soiling losses more important than ever. Using anti-soiling coatings on the PV system is a typical way of preventing soiling losses. Another option for reducing soiling losses is FPV. Since water surfaces are frequently less dusty than the arid regions where GPV is usually installed, using FPV reduces the likelihood of the panels becoming soiled. Cleaning FPV systems is usually easier than cleaning GPV systems in cases where soiling occurs, since the water at the site can be used to clean the modules.

1.9 Floating Photovoltaic Panels Hybridised with Hydropower Plants

Hydropower is a major source of electricity globally, accounting for 16% of global electricity production and 70% of renewable electricity production in 2019. However, future hydropower projects face obstacles, including environmental concerns and possible political conflicts. To maximise the potential of hydropower and reduce carbon emissions, researchers are exploring the combination of FPV systems with hydropower plants [58].

There are various benefits to combining FPV and hydropower. By restricting algae growth, it can decrease water evaporation, increase hydropower efficiency and improve water quality. FPV systems can be installed in places where connections to the electricity grid already exist, which reduces the installation cost. The intermittent nature of solar energy can be managed by combining FPV and hydropower, since the reservoir can store water even when the FPV system is not producing electricity. According to studies, hybrid FPV–hydropower systems can improve the co-production of food, energy and water.

The installation of FPV on hydropower reservoirs in various locations has been the subject of many studies. For example, installing FPV on 1% of hydropower reservoirs in Africa could increase electricity generation by 58% while reducing water evaporation. In Australia, Bangladesh and Pakistan, FPV has also shown promise in increasing electricity production and promoting sustainable development. In Brazil, the shift from hydropower to thermoelectric plants has increased greenhouse gas emissions [38]. To counteract this, Brazil must explore alternative energy sources, such as renewables.

The Alto Rabagão reservoir in Portugal, shown in Figure 1.5, has successfully used FPV and hydropower together, demonstrating the potential of coupled systems worldwide. Academic studies have highlighted the benefits of hybrid FPV–hydropower systems, making them an attractive option for addressing both environmental problems and energy needs.

Fig. 1.5: The first hybrid FPV–hydropower system, established in 2017

1.10 Irrigation Ponds

Ponds used for irrigation are a potential area for FPV installation, since the electricity obtained can be advantageous for the farms located near the irrigation ponds. Indeed, Muñoz-Cerón [44] showed that many agricultural areas require irrigation, ponds or other water-storage facilities where the installation of FPV systems is recommended, since these water bodies can also be used to produce solar energy. Because it avoids additional land purchases or permits, this can be a cost-effective alternative that reduces the cost of establishing a solar energy system. In addition, the use of FPV can have a double benefit by reducing the amount of water that evaporates from the pond, which can help conserve water resources in places where water is expensive or limited. As a result, establishing FPV on irrigation ponds can be an effective approach for producing renewable energy while preserving water resources. In Brazil, an agricultural irrigation pond was covered by a 305 kW FPV system, representing 45% of its surface [12]. Most FPV farms installed in Japan are on irrigation ponds [61]. In addition to minimising water evaporation from the ponds, the installed FPV can power the farms [45].

1.11 Salt Water versus Fresh Water

Since freshwater habitats are the main subject of FPV research and installations, salt water is considered less targeted for FPV installation, mainly because FPV systems in salt water are susceptible to elements such as tides, currents and waves in maritime regions. In addition, the complex ecology of marine ecosystems and the effects on corals must be properly taken into consideration [24]. Artificial reef creation and integration with other marine energy sources can result from FPV siting in marine environments. Figure 1.6 shows the installation of a marine FPV system in the Maldives.

Various pontoon designs are used for marine areas, such as Ocean Sun's innovative design for sheltered marine environments and Swimsol's floating SolarSea in the Maldives. In contrast with freshwater installations, marine environments also present difficulties and knowledge gaps.

Fig. 1.6: A marine FPV system in the Maldives

1.12 The Economics of Floating Photovoltaic Farms

Installing PV systems on water surfaces offers a viable alternative, especially in locations where usable land is limited, such as islands. When assessing the economic viability of power plants, the levelised cost of energy (LCOE) plays a crucial role. The LCOE takes into account various operating expenses, including fuel, maintenance and operations. Since FPV plants do not rely on fossil fuels, they are immune to fuel-price fluctuations [49].

It is important to underline that PV technology has undergone rapid progress, becoming one of the most affordable and cost-efficient sources of energy. At present, prices for PV systems are below 50 USD per megawatt-hour (USD/MWh) [25].

It is crucial to consider the expenses associated with the floating construction, which include buoys, anchoring, floats and mooring links, and which increase the total cost. Anchors can be installed on the dry banks or on the lake bottom. Inverters can be placed near a water body on dry land or, more frequently, on floats for larger installations.

The challenge arises when working with reservoirs that experience substantial fluctuations in water levels or even complete drying, since the floating structures must remain operational under such conditions. An example of this situation is Lac des Toules, an artificial reservoir located at an altitude of 1810 metres above sea level in the Swiss Alps, which is known to be drained during the winter season. The top of the reservoir hosts an FPV installation that was built in 2019. It must be able to operate in the cold climate and after the reservoir has been emptied. Other FPV examples operate in very cold environments where snowfall is likely [32], such as Harbin, Heilongjiang, China. An FPV installation built by Sungrow is another example; it was located in Taiwan and managed to withstand the typhoon season without suffering damage. Meanwhile, when submerged in water, the behaviour of PV modules is interesting: their efficiency is stronger because of the cooling effect, which also depends on depth. In addition, the module-cleaning problem was solved [50].

According to a 2018 analysis, total capital expenditure for FPV systems ranges from 0.8 to 1.2 USD/Wp [60]. With a capital cost of 0.69 USD/Wp, the Tata Power Solar installation in the West Bengal region of India illustrates how costs for large FPV plants are decreasing, with the lowest price being 0.59 USD/Wp for a 100 MW Indian plant. Asian nations dominate the FPV market in terms of capacity [23], with the largest FPV installations to be built in South Korea with a combined capacity of 2.1 GW. The largest FPV installations are currently found in China [54].

CHAPTER 2
METHODS FOR ASSESSING THE POTENTIAL OF FLOATING PHOTOVOLTAIC PANELS

2.1 Power.larc.nasa.gov

Power.larc.nasa.gov is an online portal developed by NASA (National Aeronautics and Space Administration) through the Langley Research Center. The POWER (Prediction of Worldwide Energy Resources) portal provides detailed climate and solar data for various locations around the world. These data are essential for planning and developing renewable energy projects, including photovoltaic (PV) systems, as well as for research in climatology and meteorology.

2.1.1 Main features of POWER

1. **Detailed climate and solar data:** the POWER portal offers access to a wide range of climate and solar data, including global horizontal irradiance (GHI), direct normal irradiance (DNI) – Figure 2.1 – diffuse radiation, temperatures, humidity, wind speed and other essential meteorological variables.

2. **Global coverage:** the data provided by POWER cover the entire surface of the globe, allowing users to access information for any location on the planet. This is made possible by the use of satellite data and advanced climate models.

3. **Historical time series:** users can access historical time series of data, which can be used for long-term analyses, climate studies and the evaluation of renewable energy project performance under various weather conditions.

4. **API interface:** POWER offers an API (Application Programming Interface) that allows users to access the data programmatically, facilitating their integration into software applications and data management systems.

5. **Visualisation and download tools:** the portal includes interactive data visualisation tools, such as graphs and maps, which allow users to explore and analyse the data. Users can also download data sets in various formats, such as CSV and NetCDF.

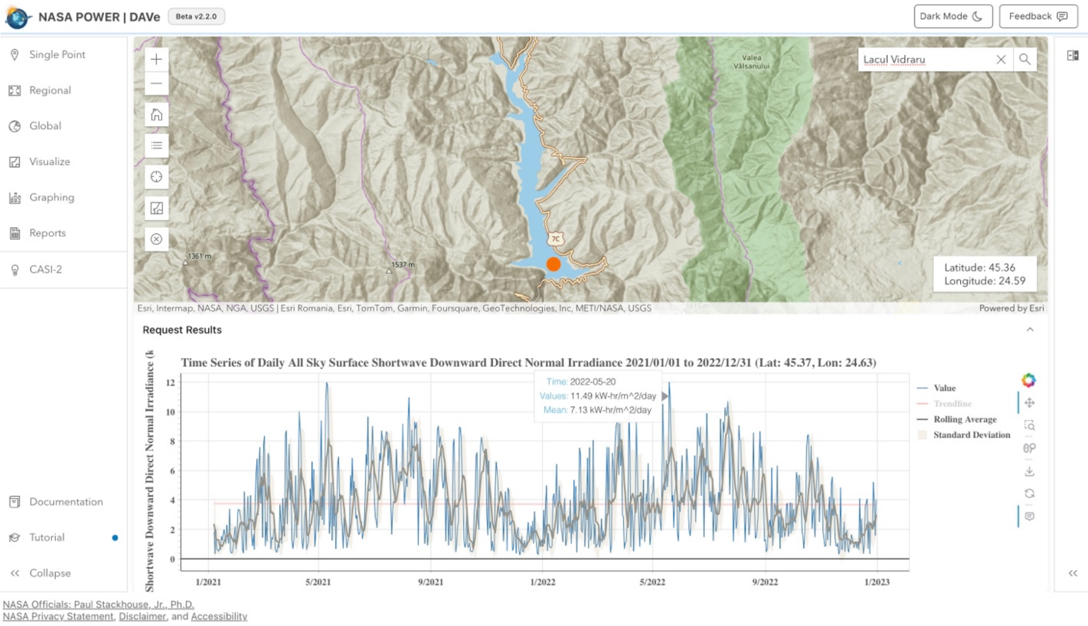

Fig. 2.1: Direct normal irradiance (DNI) over Lake Vidraru

2.1.2 Applications of POWER

1. **Renewable energy project planning:** detailed climate and solar data are essential for evaluating the energy potential of a location and for planning renewable energy projects, including photovoltaic, wind and solar thermal systems.

2. **Research and development:** researchers use the data provided by POWER for climate and meteorological studies, for the development of climate models and for assessing the impact of climate change on renewable energy resources.

3. **Education and training:** the data and tools provided by POWER are used for educational purposes, offering students and educators valuable resources for learning and research in the fields of renewable energy and climate science.

4. **Monitoring and analysis:** researchers can use historical data to monitor and analyse the performance of renewable energy systems, to identify trends and to optimise the operation and maintenance of these systems.

2.1.3 Benefits of using POWER

- **Free accessibility:** POWER is a free, online-accessible service that offers high-quality climate and solar data to users around the world.

- **Accuracy and reliability:** the data provided by POWER are based on satellite observations and advanced climate models, ensuring high accuracy and reliability.

- **Ease of use:** the intuitive interface and interactive tools make POWER easy to use, even for users without extensive technical experience.

- **Versatility:** POWER can be used for a wide range of applications, from renewable energy project planning to climate research and education.

2.1.4 How POWER works

To use the POWER portal, users access the website (power.larc.nasa.gov) and select the location of interest on the interactive map or enter its geographical coordinates. Users can then select the climate and solar variables of interest and the time interval for which they wish to obtain data. The portal then generates graphs, maps and tables with the requested data, which can be explored interactively or downloaded for later use.

2.2 Solcast.com

Solcast.com is a web platform dedicated to providing data and analytics for solar energy production. It is operated by Solcast, a technology company that uses advanced algorithms and satellite data to deliver accurate and up-to-date forecasts of solar irradiance and energy production. The Solcast.com platform is used by various industries, including energy utilities, solar project developers, grid operators and energy service providers, to manage and optimise solar resources.

2.2.1 Main features of Solcast.com

1. **Real-time solar forecasts:** Solcast provides real-time data on solar irradiance and energy production, allowing users to monitor the performance of solar installations and make quick decisions to optimise production.

2. **Advanced forecasting models:** the platform uses machine learning algorithms and advanced weather models to deliver accurate short- and long-term forecasts, covering intervals from minutes to years (Figure 2.2).

3. **Historical data:** users have access to an extensive database of historical solar irradiance data, which can be used to analyse the performance of solar systems and for future research and planning.

4. **API interface:** Solcast offers a robust API that allows easy integration of data and forecasts into users' existing systems and applications. The API provides access to forecasts, historical data and customised analyses.

5. **Monitoring and analysis:** the platform offers tools for the continuous monitoring of solar installations and for performing detailed analyses, helping users identify problems and improve operational efficiency.

6. **Customisation and scalability:** Solcast can be customised to meet the specific needs of different industries and projects, offering scalable solutions that can be adapted as projects grow.

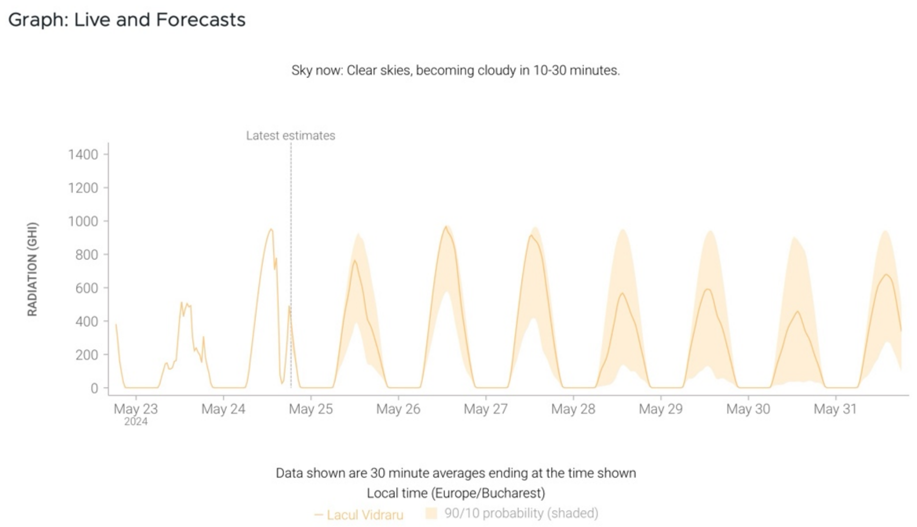

Fig. 2.2: Global Horizontal Irradiance (GHI) forecast for Lake Vidraru

2.2.2 *Applications of Solcast.com*

1. **Solar project planning and development:** Solcast data and analytics are essential for the planning and development of solar projects, helping to evaluate the solar potential and to optimise system design.

2. **Energy grid management and optimisation:** energy utilities and grid operators use Solcast forecasts to manage the integration of solar energy into distribution grids and to ensure grid stability and efficiency.

3. **Energy and commercial services:** energy service providers use Solcast data to offer customised solutions to their clients, such as dynamic tariffs, demand management and energy consumption optimisation.

2.2.3 *Benefits of using Solcast.com*

- **High accuracy:** accurate forecasts and data that help maximise solar energy production and minimise risks.

- **Operational efficiency:** tools and analyses that support quick and efficient decisions for managing solar resources.

- **Flexibility and adaptability:** customisable solutions that can adapt to the specific needs of each project or industry.

- **Accessibility:** the API interface and web platform are easy to use and integrate, providing quick access to the required data.

2.3 PVsyst

PVsyst is a professional software package used for the simulation and design of photovoltaic (PV) solar energy systems. Developed in Switzerland, PVsyst is internationally recognised and widely used by engineers, project developers, researchers and educators to evaluate the performance and the technical and economic feasibility of photovoltaic systems.

2.3.1 Main features of PVsyst

1. **PV system simulation:** PVsyst allows the detailed simulation of photovoltaic systems, including grid-connected, stand-alone and hybrid systems. Users can configure various types of solar panels, inverters and auxiliary components to create accurate models of their systems.

2. **Energy and economic analysis:** the software provides tools for the energy and economic analysis of PV projects. Users can compute the energy production, system yields and losses, as well as the economic performance by evaluating the costs and the generated revenues.

3. **Extensive weather database:** PVsyst includes an extensive meteorological database, which allows users to access historical and current data on solar irradiance and weather conditions for various locations around the world. Users can also import meteorological data from external sources.

4. **Design and optimisation:** the design tools in PVsyst allow users to create and optimise PV system configurations. This includes the optimal sizing of components, the evaluation of panel orientation and tilt, and the analysis of shading effects.

5. **Performance evaluation:** PVsyst provides detailed reports on the performance of PV systems, including production, loss and efficiency analyses. The reports are customisable and can be used to communicate simulation results to stakeholders.

6. **Component library:** the software includes an extensive component library, comprising solar panels, inverters, batteries and other equipment. Users can add new components or modify the characteristics of existing ones to reflect actual product specifications.

7. **Detailed system modelling:** PVsyst allows the detailed modelling of PV system components, including photovoltaic modules, inverters, cables, transformers and other equipment. This enables an accurate simulation of system performance under various operating conditions.

2.3.2 Applications of PVsyst

1. **Design and engineering:** engineers and project developers use PVsyst to design and optimise photovoltaic systems, making sure they meet the technical and economic requirements of their projects.

2. **Feasibility analyses:** PVsyst is used to carry out technical and economic feasibility analyses, helping investors and developers make informed decisions about the viability of PV projects.

3. **Research and education:** researchers and educators use PVsyst to study the performance of photovoltaic systems and to teach concepts related to solar energy and PV system design.

4. **Monitoring and evaluation:** PVsyst can be used to monitor and evaluate the performance of existing PV systems, identifying potential problems and opportunities to improve efficiency.

2.3.3 Benefits of using PVsyst

- **Accuracy and reliability:** the simulations and analyses provided by PVsyst are recognised for their accuracy and reliability, being widely used in the industry.
- **Versatility:** the software can be used for a wide range of applications, from small residential projects to large commercial and utility-scale projects.
- **Advanced tools:** PVsyst offers advanced tools for the simulation and optimisation of PV systems, allowing users to obtain accurate and detailed results.
- **Support and documentation:** PVsyst benefits from technical support and detailed documentation, including tutorials and guides, which help users learn and use the software efficiently.

2.4 PVGIS

PVGIS (Photovoltaic Geographical Information System) is an online tool developed by the European Commission through the Joint Research Centre (JRC). PVGIS provides detailed and accurate estimates of solar resources and photovoltaic system performance for locations around the world. It is widely used by engineers, researchers, solar project developers and other professionals in the solar energy field.

2.4.1 Main features of PVGIS

1. **Solar resource estimation:** PVGIS provides accurate solar irradiance data for specific locations, using historical data and advanced models. These data include global horizontal irradiance (GHI), direct normal irradiance (DNI) and irradiance on a tilted surface (Figure 2.3).
2. **PV system performance simulation:** the tool allows the simulation of photovoltaic system performance for different system configurations and locations. Users can specify parameters such as the orientation and tilt of the solar panels and the module and inverter types, and can obtain energy production estimates.
3. **Loss and yield analyses:** PVGIS provides detailed analyses of energy losses in PV systems, including temperature losses, optical losses, cable losses and other systematic losses. It also computes the system yield and the capacity factor.
4. **Weather databases:** the tool uses several meteorological databases, such as CM-SAF, ERA5 and SARAH, to provide users with high-quality data on weather conditions and solar resources (Figure 2.4).
5. **Visualisation tools:** PVGIS includes visualisation tools that allow users to explore solar maps, production diagrams and other graphical representations of the data. These visualisations help in understanding the distribution of solar irradiance and the performance of PV systems.

6. **Reporting and data export:** users can generate detailed reports that include all simulation results and analyses. Data can be exported in various formats, including PDF and CSV, for later use.

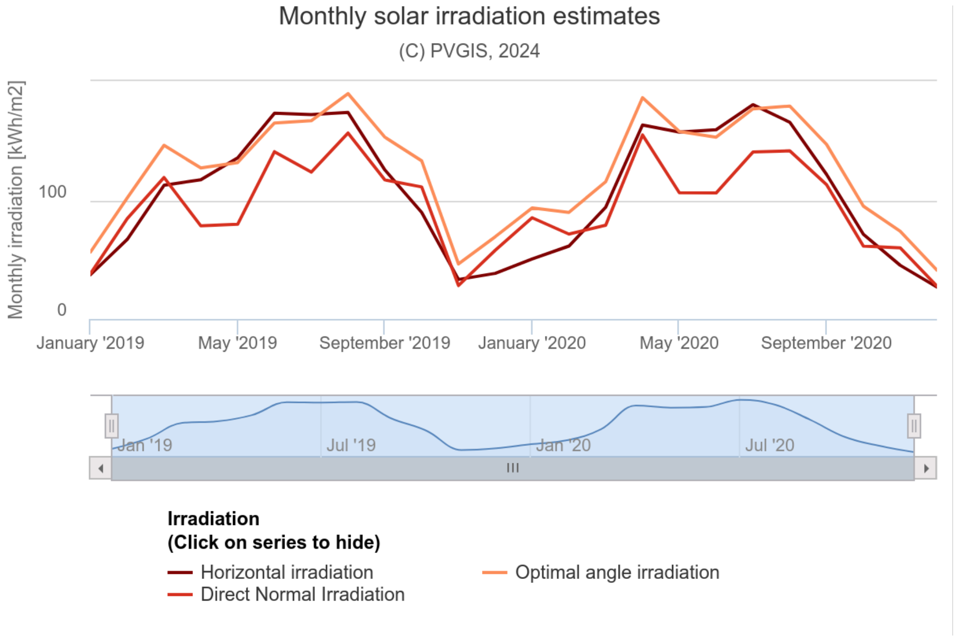

Fig. 2.3: Global horizontal irradiance (GHI), direct normal irradiance (DNI) and irradiance on a tilted surface for Lake Vidraru

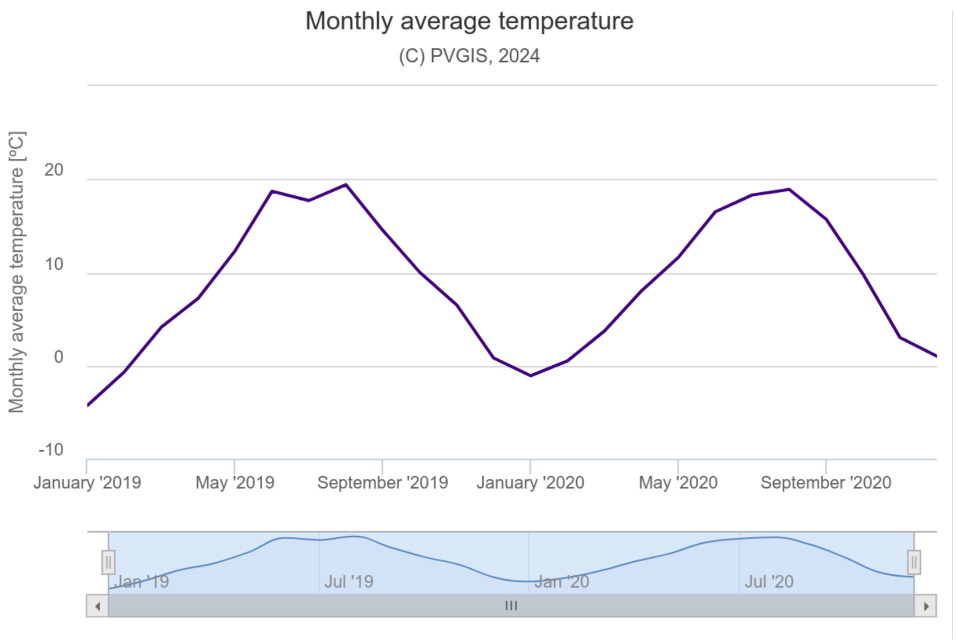

Fig. 2.4: Average monthly temperature in the Lake Vidraru area

2.4.2 Applications of PVGIS

1. **Solar project planning:** PVGIS is used to evaluate the solar potential of a location and to estimate the energy production of a PV system. This information is essential for the

correct planning and sizing of solar projects.

2. **Research and development:** researchers use PVGIS to study solar resources and the performance of photovoltaic systems under various conditions and locations. The tool is also used for the development of new technologies and solutions in the field of solar energy.

3. **Education and training:** PVGIS is a valuable tool for educators and students, providing an interactive platform for learning solar energy concepts and for carrying out practical studies and projects.

4. **Economic analyses:** although PVGIS focuses on technical aspects, its energy production estimates are also useful for economic analyses, helping to compute the costs and benefits of PV projects.

2.4.3 Benefits of using PVGIS

- **Free accessibility:** PVGIS is a free, online-accessible tool, which makes it available to a wide audience, including professionals, researchers and students.
- **Accuracy and reliability:** the use of high-quality meteorological databases and advanced models ensures the accuracy and reliability of the estimates provided by PVGIS.
- **Ease of use:** the intuitive interface and the visualisation tools make PVGIS easy to use, even for those without extensive technical experience.
- **Versatility:** PVGIS can be used for a wide range of applications, from residential solar project planning to the analysis of large commercial and industrial systems.

2.4.4 How PVGIS works

To use PVGIS, users access the website and select the location of interest on the interactive map. They then enter the PV system parameters, such as the module type, the tilt and orientation of the panels, and other technical specifications. PVGIS then computes the estimated energy production, the system losses and other relevant metrics, providing detailed results and graphical visualisations.

2.5 SolarAtlas

SolarAtlas is an online tool developed by various solar data service providers and organisations to offer detailed information about the solar resources available at a given location. It is used to evaluate the solar energy potential, to support the planning and development of photovoltaic (PV) projects and to provide essential data to researchers and project developers. SolarAtlas relies on high-quality meteorological and solar data and uses advanced modelling technologies to deliver accurate estimates of solar irradiance and PV system performance.

2.5.1 Main features of SolarAtlas

1. **Solar resource estimation:** SolarAtlas provides detailed solar irradiance data, including global horizontal irradiance (GHI), direct normal irradiance (DNI) and diffuse irradiance. These data are essential for evaluating the solar potential of a location.

2. **PV system performance simulation:** the tool allows users to simulate the performance of photovoltaic systems, taking into account parameters such as the orientation and tilt of the solar panels, the PV module type and the inverter type. This helps estimate the electricity production for various system configurations.

3. **High-quality meteorological data:** SolarAtlas uses high-quality meteorological data from weather stations, satellites and climate models. These data are updated regularly to ensure the accuracy and relevance of the estimates.

4. **Visualisation tools:** SolarAtlas offers interactive maps and graphs that allow users to visualise the distribution of solar irradiance and the performance of PV systems in a given region. These visualisations help identify the optimal locations for installing solar systems (Figure 2.5).

5. **Detailed loss and yield analyses:** the tool provides detailed analyses of energy losses in PV systems, including losses due to temperature, shading, soiling and other factors. It also computes the system yield and the capacity factor.

6. **Data export and reporting:** users can generate detailed reports and export data in various formats to be used in further analyses or presentations, or for integration with other tools and software applications.

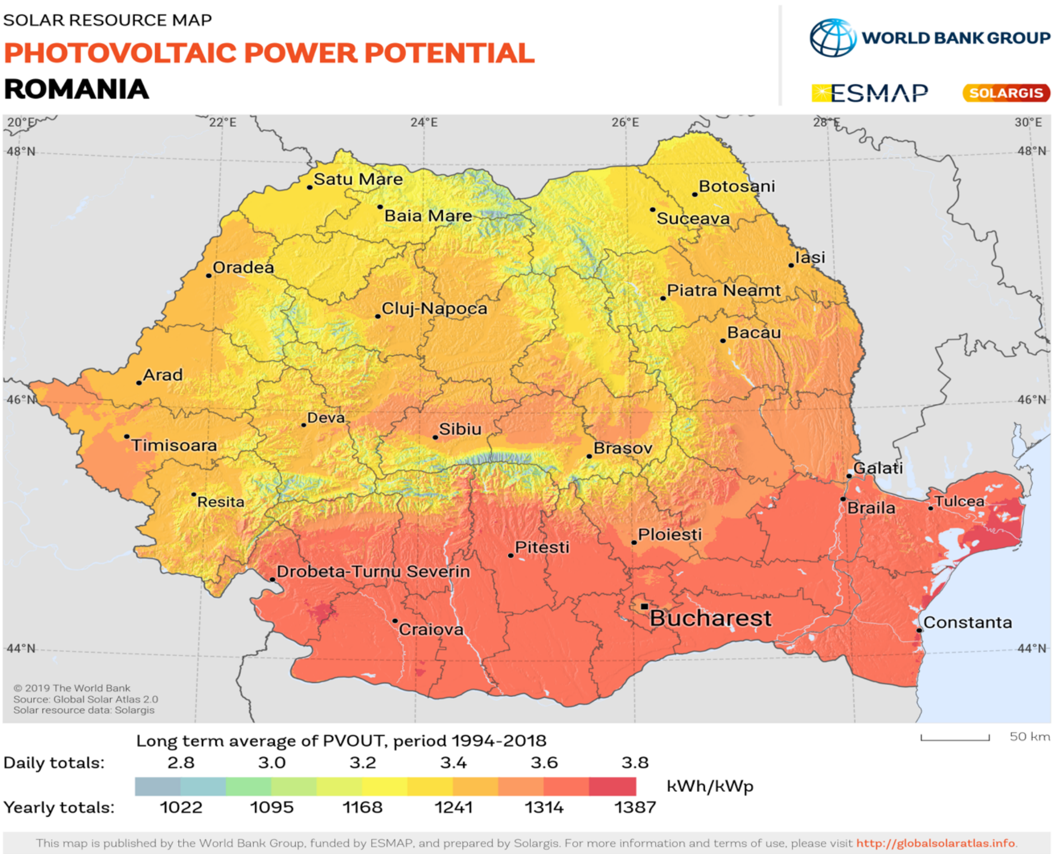

Fig. 2.5: Map of the photovoltaic potential over the territory of Romania

2.5.2 Applications of SolarAtlas

1. **Solar project planning and development:** SolarAtlas is used for solar resource assessment and for estimating the energy production of PV systems. This information is essential for the correct planning and sizing of solar projects, whether residential, commercial or industrial.

2. **Feasibility analyses:** project developers and investors use SolarAtlas to carry out technical and economic feasibility analyses, evaluating the energy potential and the profitability of investments in solar projects.

3. **Research and education:** researchers and educators use SolarAtlas to study solar resources and the performance of photovoltaic systems. It is an important instrument for carrying out educational studies and projects in the field of renewable energy.

4. **Energy policy and urban planning:** governments and local authorities can use SolarAtlas to develop energy policies and to plan the development of solar infrastructure in specific regions, promoting the use of renewable energy and the reduction of carbon emissions.

2.5.3 Benefits of using SolarAtlas

- **Accessibility:** SolarAtlas is usually available online and can be accessed free of charge or for a fee, depending on the service provider. This facilitates access to high-quality solar data for a wide audience.

- **Accuracy:** the use of high-quality meteorological and solar data ensures the accuracy of the estimates provided by SolarAtlas, helping the efficient planning of PV projects.
- **Ease of use:** the intuitive interface and the visualisation tools make SolarAtlas easy to use, even for users without extensive technical experience.
- **Versatility:** SolarAtlas can be used for a wide range of applications, from small residential projects to large commercial and utility-scale projects.

2.5.4 How SolarAtlas works

To use SolarAtlas, users access the website and select the location of interest on the interactive map. They then enter the PV system parameters, such as the module type, the tilt and orientation of the panels, and other technical specifications. SolarAtlas then computes the estimated energy production, the system losses and other relevant metrics, providing detailed results and graphical visualisations.

CHAPTER 3
DESCRIPTION OF THE SELECTED SITES

In this case study, we selected the placement of floating photovoltaic panels on the hydropower reservoir lakes with the largest surface areas in Romania. Figure 3.1 shows the six analysed lakes on the map of Romania: Izvorul Muntelui, Vidra, Vidraru, Goleşti, Oaşa and Colibiţa.

In addition to the benefits listed in Chapter 1 (Section 1.7, Performance and Efficiency of Floating Photovoltaic Panels), combining floating solar systems with hydropower systems on reservoir lakes promotes synergies in their integration into the energy system by using the existing grid connections. Implementing FPV (floating photovoltaic panels) on hydropower reservoirs can optimise energy generation and increase system reliability compared with land-based PV systems, owing to the cooling effect of the water. Using the existing hydropower infrastructure, such as transmission extensions and substations, can reduce the costs and time required for obtaining licences and purchasing land.

In order to optimise hydropower operation and water resource management, the analysis of the prevailing wind directions was also taken into consideration. These data are essential for the design and operation of flood-control infrastructure, since the direction and intensity of the winds can influence the water level and its distribution in the reservoir.

Winds can also affect water evaporation, which is crucial for maintaining the optimal capacity of the reservoir.

The wind rose (Figures 3.2–3.7) is also important for the installation and operation of floating photovoltaic panels. The direction and intensity of the winds influence the stability and efficiency of these panels, contributing to the optimisation of solar energy capture.

We used a Python script to retrieve wind speed and direction data from the NASA POWER API at a height of 2 metres.

Given that the wind speed and direction parameters are provided at a height of 2 metres, in order to adjust these data to a height of 1 metre we used the power-law formula:

$$V_h = V_{\text{ref}} \times \left(\frac{h}{h_{\text{ref}}} \right)^{\alpha} \tag{3.1}$$

where α (the power-law coefficient) was set to 0.12, a value specific to reservoir lakes. This allowed us to estimate the wind speed at 1 metre starting from the 2-metre data, and to generate the wind roses.

Fig. 3.1: Location of the reservoir lakes

3.1 The Izvorul Muntelui Hydropower Complex

The Bistriţa River is the first river in Romania to have been fully developed along its middle and lower course through the construction of a large reservoir, the "Izvorul Muntelui" reservoir, with the main power plant "Dimitrie Leonida" ("Bicaz") – where a large part of the river's flow and head difference is concentrated – and 12 small hydropower plants downstream of it. Through the Izvorul Muntelui reservoir, the requirements of various complex purposes can be fulfilled: hydropower, irrigation, water supply, and flood control at 50–60% of their natural value. Its active capacity represents 65% of the possible storage capacities within the river basin.

The development comprises the following structures:

- a concrete gravity dam located approximately 30 km upstream of the town of Piatra Neamţ;
- a water intake located 1.5 km upstream of the dam, on the left bank, ensuring the entry of water from the reservoir into the headrace tunnel;
- a 480 m long headrace tunnel, with an internal diameter of 7 m;
- a penstock composed of two pipes;
- a power plant.

Table 3.1: Technical data of the Izvorul Muntelui Hydropower Complex

Technical data	
Development	
River: Bistriţa	Nearest town: Piatra Neamţ
County: Neamţ	Hydropower complex: Izvorul Muntelui
Catchment area: 4025 km^2	Construction period: 1950–1960
Dam–Reservoir	
Maximum dam height: 127 m	Crest length: 435 m
Crest width: 10.10 m	Maximum base width: 119 m
Excavated material volume: 520,000 m^3	Dam volume: 1,625,000 m^3
Reservoir capacity at NRL: 1,230×10^6 m^3	Reservoir area at NRL: 31,170,000 m^2
Normal retention level: 513.00 m a.s.l.	Minimum operating level: 470 m a.s.l.
Main purposes	
Hydropower: gross head 125 m; installed power 210 MW; energy production 435 GWh/year	
Irrigation	
Flood control	

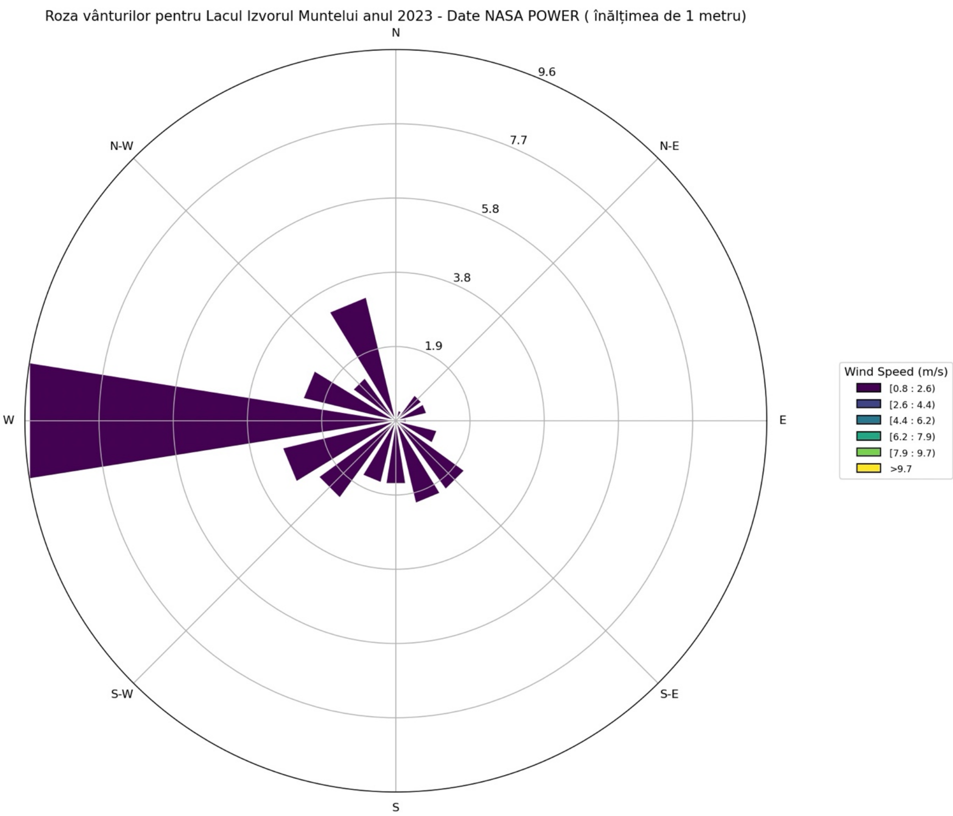

Fig. 3.2: Wind rose for Lake Izvorul Muntelui

3.2 The Lotru Hydropower Complex – the Vidra Reservoir

The Lotru hydropower development is located in the Southern Carpathians, on the southern slopes of the Cibin, Lotru and Căpăţâna mountains and in the easternmost part of the Parâng massif, being placed in the middle of the crystalline massif. The Vidra Dam was built to create the main reservoir within the hydropower development scheme of the Lotru River basin. The hydropower development of the Lotru River is of particular importance in the general context of developments in Romania because, owing to its many kilometres of secondary galleries, it concentrates the flows from neighbouring basins into a single reservoir.

The development scheme consists of two distinct parts:

- the main reservoir formed by the Vidra Dam, the water intake, the headrace gallery, the surge chamber, the butterfly-valve building, the pressure gallery, the spherical-valve building, the underground Ciunget power plant, the transformer hall with its access gallery and cable gallery, the tailrace gallery and the adjacent structures;
- the network of secondary intakes and galleries through which the waters of the Lotru basin and of the neighbouring river basins are collected and conveyed by gravity or by pumping to the Vidra reservoir. Downstream of the Ciunget hydropower plant there are also two power plants: Mălaia and Brădişor.

The Lotru basin is characterised by ample precipitation of the order of 1160 mm/year, compared with the average mountain conditions in Romania of 670 mm/year.

The mean specific discharge is 26 l/s/km^2.

The maximum discharges for various probabilities were computed on the basis of the records made at the hydrometric stations in the Lotru River basin, with the characteristics of the flood hydrographs established according to the analysis of the main floods recorded at these hydrometric stations between 1950 and 1994. For the Vidra Dam, the design discharge was the maximum discharge with an exceedance probability of 0.1%, equal to 470 m^3/s, while the check discharge, the one with an exceedance probability of 0.01% adjusted by 20%, amounts to 745 m^3/s.

The suspended-sediment discharge, established according to the hydrological data recorded at the hydrometric stations, is 100 g/m^3, on the basis of which the mean annual suspended-sediment discharge in the reference sections is computed.

Table 3.2: Technical data of the Lotru Hydropower Complex

Technical data	
Development	
River: Lotru	Nearest town: Brezoi
County: Vâlcea	Hydropower complex: Izvorul Lotru
Catchment area: 167 km^2	Construction period: 1966–1973
Dam–Reservoir	
Maximum dam height: 121 m	Crest length: 350 m
Crest width: 10 m	Maximum base width: 450 m
Excavated material volume: 260,000 m^3	Dam volume: 3,550,000 m^3
Reservoir capacity at NRL: 11,250×10^3 m^3	Reservoir area at NRL: 31,170,000 m^2
Normal retention level: 1289 m a.s.l.	Minimum operating level: 1237 m a.s.l.
Main purposes	
Hydropower: gross head 809 m; installed power 510 MW; energy production 1100 GWh/year	

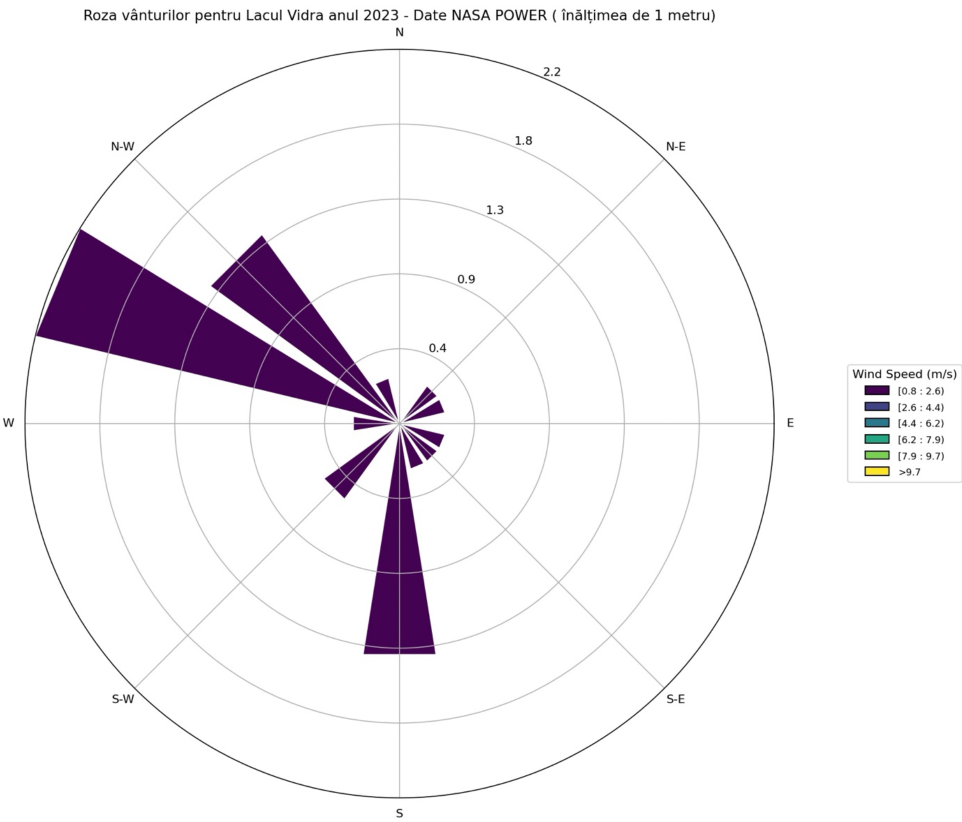

Fig. 3.3: Wind rose for Lake Vidra

3.3 The Argeş Hydropower Development – Lake Vidraru

The Argeş hydropower station is developed on the Argeş River sector between Cumpăna and Oieşti, over a length of approximately 27 km, and comprises the following structures:

- a concrete arch dam located in the Argeş Gorge at Vidraru;
- a pressurised headrace gallery, from the dam to the power plant, with a length of 2.13 km;
- the surge chamber;
- an underground power plant;
- a free-flow tailrace gallery 11.13 km long;
- a system of secondary intakes for diverting additional flows into the Vidraru reservoir.

The specific multiannual mean discharges vary between limits of over 40 l/s/km^2 at high altitudes and below 1 l/s/km^2 in the Danube Plain. The maximum discharges are caused by torrential rains; the flood waves have a violent character, reaching a specific peak discharge of over 2 m^3/s/km^2 at an exceedance probability of 0.1% for small high-altitude basins. The washed layer generating suspended sediment is minimal in the upper and lower parts of the basin (below 50 t/km^2/year) and maximal in the hilly area (over 10 t/ha/year). The mean turbidity fluctuates between 500 g/m^3 and 2000 g/m^3.

Hydrometric measurements in the Argeş River basin down to Piteşti were carried out at 40 hydrometric stations, of which 10 are equipped with water-level recorders.

Table 3.3: Technical data of the Argeş Hydropower Complex – Lake Vidraru

Technical data	
Development	
River: Argeş	Nearest town: Curtea de Argeş
County: Argeş	Hydropower complex: Argeş
Catchment area: 286 km^2	Construction period: 1960–1965
Dam–Reservoir	
Maximum dam height: 166 m	Crest length: 305 m
Crest width: 6 m	Maximum base width: 25 m
Excavated material volume: 147,500 m^3	Dam volume: 470,000 m^3
Reservoir capacity at NRL: 469×10^6 m^3	Reservoir area at NRL: 10,000,000 m^2
Normal retention level: 830 m a.s.l.	Minimum operating level: 778 m a.s.l.
Main purposes	
Hydropower: gross head 324 m; installed power 220 MW; energy production 400 GWh/year	
Irrigation of 100,000 hectares	
Water supply for Bucharest	

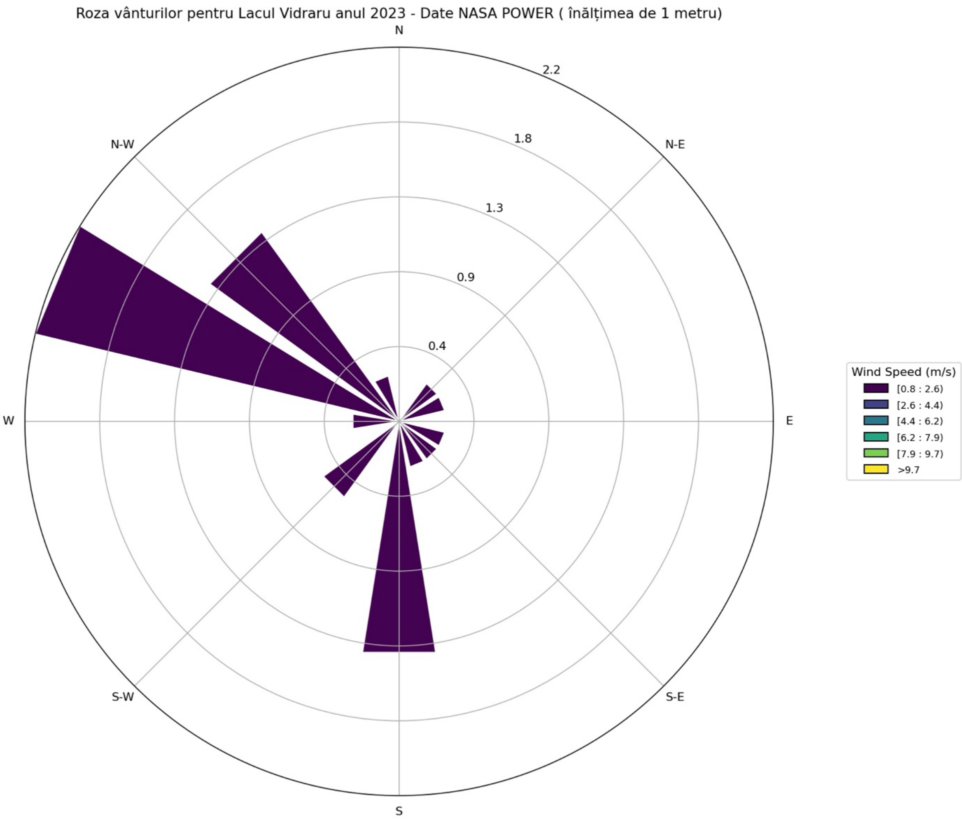

Fig. 3.4: Wind rose for Lake Vidraru

3.4 The Argeş Hydropower Complex – Lake Goleşti

Hydrotechnical development

This development is included in the water development and management scheme of the Argeş River, whose basin accommodates a population of over two million inhabitants. The scheme consists of 17 dams and reservoirs storing a water capacity of 0.485 km^3/year (Vidraru, Budeasa, Goleşti etc.), and its purpose is to generate electricity, to provide an additional flow for the water supply of the city of Bucharest, to supply irrigation water for the fertile lands and to provide flood control. For these reasons, the Goleşti reservoir is part of a dispatching system for the water supply of Bucharest, the capital of Romania. The Argeş River ranks first in terms of sediment transport, and the five reservoirs are largely silted. For the Goleşti Dam, a construction solution was designed to allow the transfer of the sediment stock downstream; this required the construction of a discharge structure with a flow capacity of over 2,000 m^3/s through the bottom outlets, considering that flood discharge is to take place at levels closer to the natural regime, thereby maintaining a relatively constant balance between erosion and sediment deposition.

The Goleşti hydrotechnical development includes the following main works: a gated dam, a longitudinal dam located on the left bank of the Argeş River, a hydropower plant located on the right side of the discharge front, as well as other adjacent works (a water pumping station for the irrigation systems; a water pumping station for the back-up supply of the Piteşti industrial area; a drainage and collection channel for the Ştefăneşti, Văleni and Vrăneşti valleys, parallel to the longitudinal dam; the development of the Argeş River).

Downstream of the Goleşti Dam

Over a length of approximately 600 m: the raising of the dykes bordering the tailrace channel of the Prundu hydropower plant, Piteşti; hydromechanical equipment; monitoring devices and instrumentation for supervising the behaviour of the works over time; electrical and telephone systems; an operating unit; the consolidation of the right bank upstream and downstream of the frontal dam.

Hydrology

The main characteristic of the Argeş River basin is the fact that both the basin area and the hydrological potential of the river are concentrated in the upper (mountainous and hilly) part of the basin, with direct consequences for flood generation.

Between October 1972 and July 1983, many floods occurred, generating significant material losses in the lower area of the Argeş River basin. This was due to the storage capacities existing at the time, which had low protection surcharges for flood routing (with the exception of the Vidraru reservoir); moreover, there were no reservoirs on the Doamnei River.

Following the floods of the aforementioned period, the possible maximum discharges were substantially revised and, in the design of the Goleşti storage works, the following values were taken into account in the computations: $Q_{5\%}$ = 1,360 m^3/s; $Q_{1\%}$ = 2,180 m^3/s; $Q_{0.1\%}$ = 3,760 m^3/s; $Q_{0.01\%}$ = 5,600 m^3/s; the multiannual mean discharge $Q_{m.a.}$ = 36.50 m^3/s.

An important characteristic of the Argeş River, especially downstream of the Doamnei River, is the transport of large sediment loads, estimated at approximately 2.0–2.5 million tonnes annually.

Table 3.4: Technical data of the Argeş Hydropower Complex – Lake Goleşti

Technical data	
Development	
River: Argeş	Nearest town: Piteşti
County: Argeş	Hydropower complex: Argeş
Catchment area: 3100 km^2	Construction period: 1978–1984
Dam–Reservoir	
Maximum dam height: 32 m	Crest length: 616 m
Crest width: 9 m	Maximum base width: 136 m
Excavated material volume: 360,000 m^3	Dam volume: 280,000 m^3
Reservoir capacity at NRL: 78×10^6 m^3	Reservoir area at NRL: 6,800,000 m^2
Normal retention level: 251 m a.s.l.	Minimum operating level: 245 m a.s.l.
Main purposes	
Hydropower: gross head 11.5 m; installed power 8 MW; energy production 33 GWh/year	
Irrigation of 100,000 hectares	
Water supply for the Arpechim petrochemical complex	
Flood protection for an area of 500 km^2	

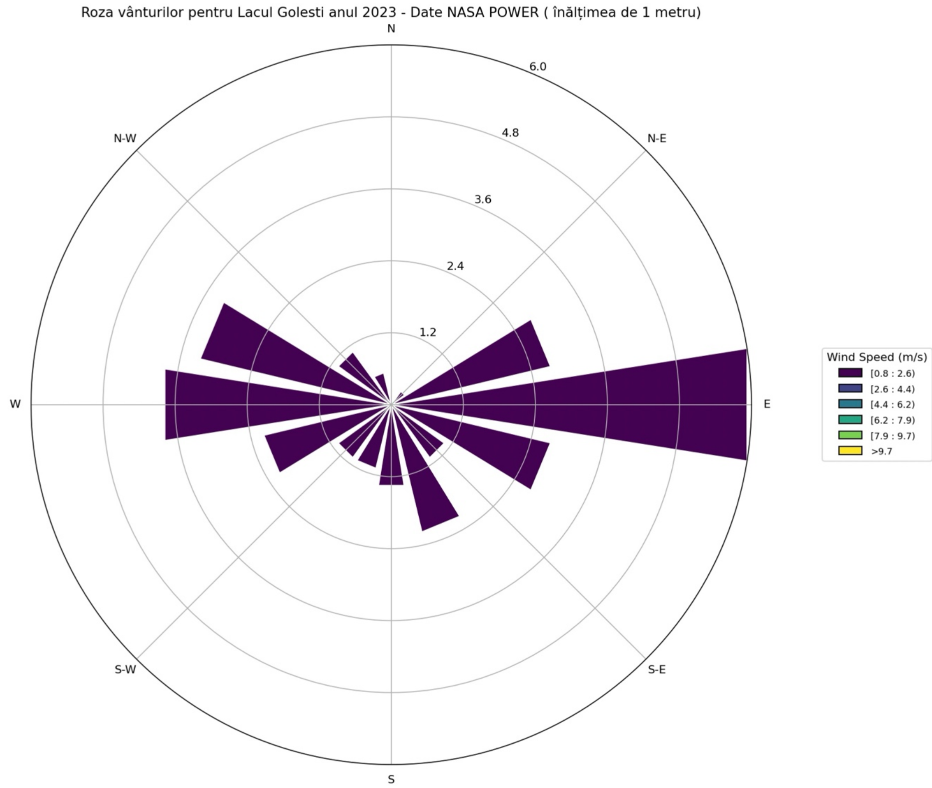

Fig. 3.5: Wind rose for Lake Goleşti

3.5 The Sebeş Hydropower Complex – Lake Oaşa

The development of the Sebeş River, which has a total length of 93 km, is located in the Southern Carpathians, with a total catchment area of 1290 km^2.

The Oaşa Dam creates the main reservoir within the hydropower development scheme of the Sebeş River. The right-bank tributaries – Bistra, Tortura, Ruginosu and Mărginea – are also captured into the reservoir through a 12.3 km secondary headrace gallery.

A dam on the Cugirul Mare is under construction, with a 6.5 km headrace gallery and a 20 MW pumping station upstream of the Gâlceag power plant.

The catchment of the Sebeş River at the Oaşa section has an area of 187 km^2, a river length of 22 km and a mean basin altitude of 1570 m above sea level (a.s.l.).

The mean discharge captured at the Oaşa section is 5.42 m^3/s. The Cugir and Gâlceag basins will bring an additional contribution of 2.21 m^3/s.

The suspended-sediment discharge is 0.5 kg/s, while the bed-load sediment transport is 0.8 kg/s.

According to the standards, the dam is included in the second importance class; therefore, the spillway should allow the discharge of a check flow of $1.2 \times Q_{0.1\%}$.

The Oaşa Dam site is located in the micaceous gneiss area of the Sebeş–Lotru zone. This gneiss has lateral transitions towards mica schists. The whole complex is sometimes penetrated by pegmatite lenses and veins and shows an advanced degree of weathering and tectonisation. Weathering is more pronounced on the left bank as a result of the schistosity orientation, the tectonic lines and the freeze–thaw cycles.

The direction of the schistosity is approximately perpendicular to the valley, with a dip of 10°–40° towards upstream; the exception lies in a restricted area on the right bank where the dip is towards downstream. Faults are frequent along the entire dam area and generally have N–S and NW–SE directions, with dips between 30° and 80°. The main faults have led to local disturbances of the schistosity (especially in the left-bank area above elevation 1230 m a.s.l.) through micro-folding, fracturing and cracking accompanied by severe weathering that has locally reached the stage of argillisation.

Table 3.5: Technical data of the Sebeş Hydropower Complex

Technical data	
Development	
River: Sebeş	Nearest town: Sebeş
County: Alba	Hydropower complex: Sebeş
Catchment area: 187 km^2	Construction period: 1973–1979
Dam–Reservoir	
Maximum dam height: 91 m	Crest length: 300 m
Crest width: 10 m	Maximum base width: 282 m
Excavated material volume: –	Dam volume: 1,680,000 m^3
Reservoir capacity at NRL: 136×10^6 m^3	Reservoir area at NRL: 4,010,000 m^2
Normal retention level: 1255 m a.s.l.	Minimum operating level: 1206 m a.s.l.
Main purposes	
Hydropower: gross head 465 m; installed power 150 MW; energy production 260 GWh/year	

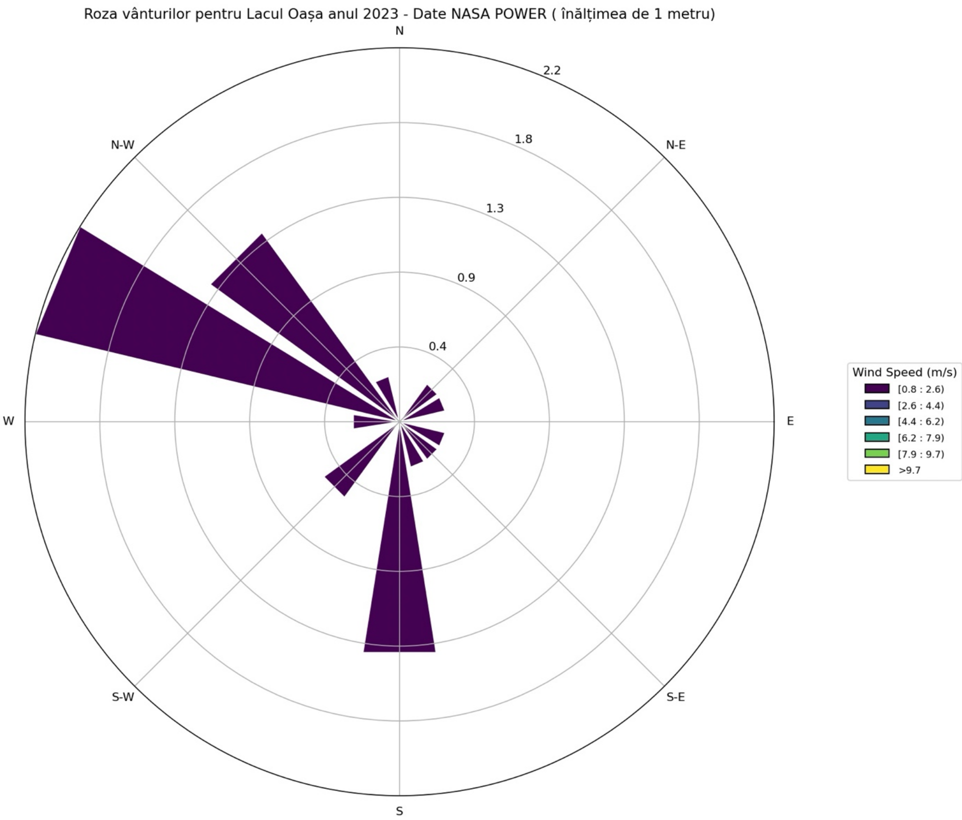

Fig. 3.6: Wind rose for Lake Oaşa

3.6 The Colibiţa Hydropower Complex

The Colibiţa Dam is located in the upper basin of the Someş River, approximately 40 km upstream of the town of Bistriţa, Bistriţa-Năsăud County. It is a rockfill dam with a bituminous concrete face. The dam was designed for a discharge with an exceedance probability of 0.1‰, namely 490 m^3/s, while the check was carried out for a discharge of $1.2 \times Q_{0.01\text{‰}}$, namely 990 m^3/s. The mean captured discharge is 2.2 m^3/s, and the mean discharges captured from other basins through secondary diversions amount to 1.6 m^3/s. The partial commissioning of the dam took place in 1982, with a water volume of $10{\times}10^6$ m^3, at approximately 50% of its height. The face was executed mechanically over its entire surface. For the last 4 metres of the dam height, a retaining-wall solution was adopted. The base of the wall is located at an altitude of 802.00 m above sea level, and its crest at 806.00 m above sea level. This wall also has the role of breaking the waves.

The volcanic breccia is represented by andesite blocks and elements of various shapes and sizes, embedded in a mass of volcanic ash and lava cement, with interlayers of andesite lava or friable sandy clay. The large fluctuations in the thickness of the andesite layer (20–80 m) along the valley, which match a pre-existing relief, show that this slab is fragmented by tectonic accidents whereby the various blocks have been subjected to uplifts and subsidences of varying amplitudes over time. Below this layer of agglomerates and volcanic breccia lies the Helvetian–Tortonian sedimentary formation, represented by marls, clays, sandstones and tuffs. The general structure of the sedimentary formations is a monocline with a NW–SE direction and a dip towards SW of 20°–30°. The contact between the agglomerates and the underlying sedimentary rock is most often accompanied by crushing phenomena, and it is assumed that, in addition to the phenomena of vertical uplift and subsidence, there were also phenomena of falling and translation of the various parts. The predominant direction of the agglomerate–sedimentary contact is NW–SE, with a dip towards SW of 25°–35°. The dam is located in a microseismic zone of intensity $I = 6$ (MSK), with a seismicity coefficient $K = 0.06$ and a control period equal to 0.7 s.

Table 3.6: Technical data of the Colibiţa Hydropower Complex

Technical data	
Development	
River: Bistriţa Ardeleană	Nearest town: Bistriţa
County: Bistriţa-Năsăud	Hydropower complex: Colibiţa
Catchment area: 113 km^2	Construction period: 1976–1993
Dam–Reservoir	
Maximum dam height: 92 m	Crest length: 250 m
Crest width: 10 m	Maximum base width: 288.5 m
Concrete volume: 18,000 m^3	Dam volume: 1,610,000 m^3
Reservoir capacity at NRL: 136×10^6 m^3	Reservoir area at NRL: 75,220,000 m^2
Normal retention level: 797.45 m a.s.l.	Minimum operating level: 740.00 m a.s.l.
Main purposes	
Hydropower: gross head 194.5 m; installed power 21 MW; energy production 47.5 GWh/year	
Water supply for the localities downstream of the hydropower plant (4.2 m^3/s)	
Flood protection	

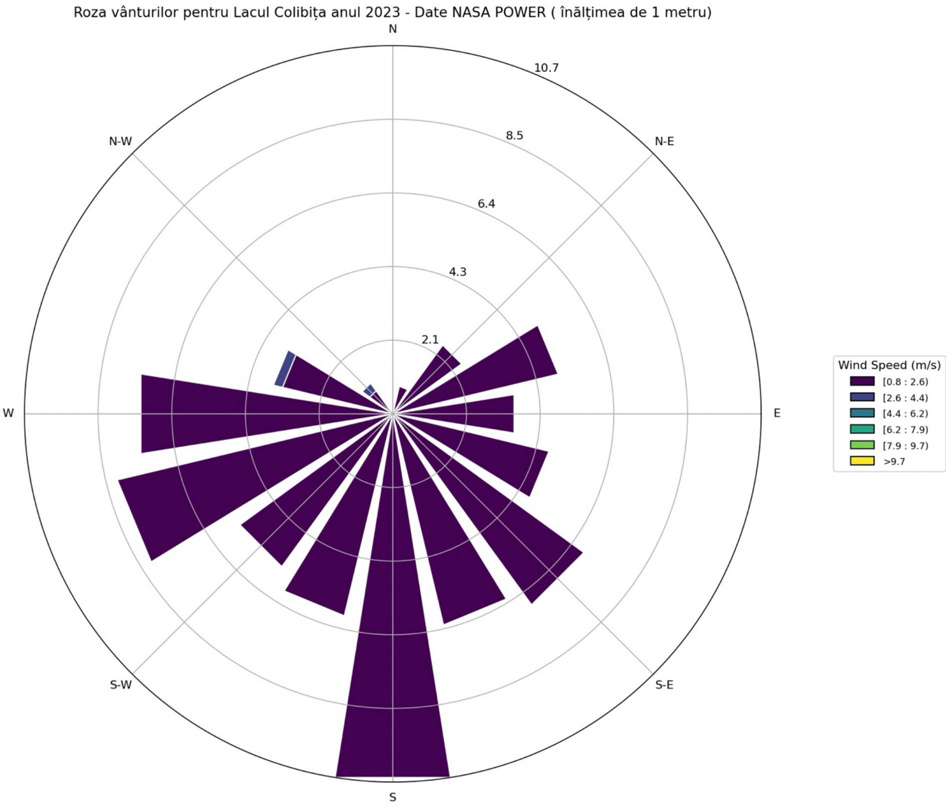

Fig. 3.7: Wind rose for Lake Colibiţa

CHAPTER 4
ASSESSMENT OF THE SOLAR POTENTIAL OVER RESERVOIR LAKES USING GEOSPATIAL TECHNIQUES

This study was carried out in order to evaluate the solar potential over reservoir lakes. Remote sensing techniques, a geographic information system (GIS) and the cloud environment were applied to assess the solar potential available over the reservoir lakes presented in the previous chapter. Satellite imagery from Google Earth was downloaded in order to extract the usable area for floating photovoltaic panels (FPV) over the lakes. The global horizontal irradiance (GHI) and the direct normal irradiance (DNI) were retrieved through a script written in the Python programming language using the APIs (Application Programming Interfaces) of the Power.larc.nasa.gov website, an online portal developed by NASA (National Aeronautics and Space Administration) through the Langley Research Center, for the computations. These DNI and GHI values were converted into tilted GHI in order to obtain an accurate assessment of the solar potential. A Python script was developed to convert GHI into tilted GHI.

In the present study, the solar irradiation potential of floating photovoltaic panels (FPV), tilted at angles of 45 and 10 degrees respectively, was evaluated on the reservoir lakes presented in the previous chapter: Izvorul Muntelui (Bicaz), Vidra, Goleşti, Colibiţa, Oaşa and Vidraru.

4.1 Study Areas

The selected study areas are the reservoir lakes presented in the previous chapters (Figures 4.1–4.6).

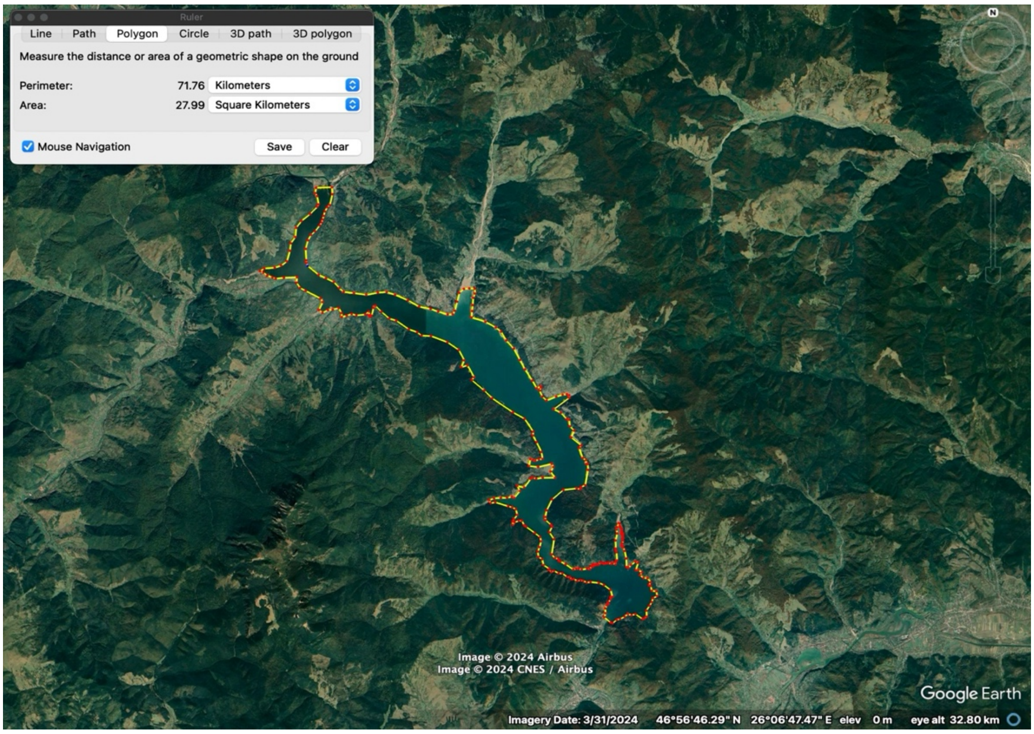

Fig. 4.1: The Izvorul Muntelui reservoir lake

Fig. 4.2: The Vidra reservoir lake

Fig. 4.3: The Goleşti reservoir lake

Fig. 4.4: The Colibiţa reservoir lake

Fig. 4.5: The Oaşa reservoir lake

Fig. 4.6: The Vidraru reservoir lake

4.2 Computation Methodology

The methodology adopted for this study is presented in Figure 4.7.

Google Earth Pro was used to download the satellite images and to extract the geographical data, namely the latitude and the longitude.

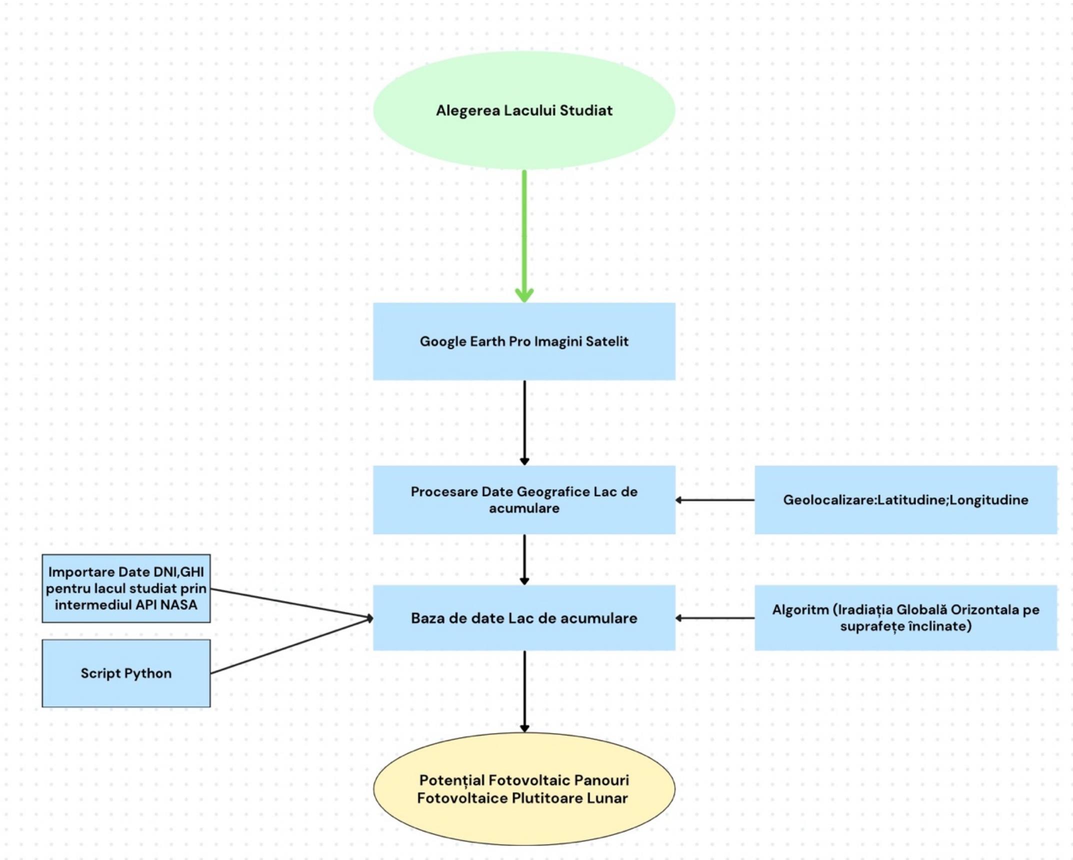

Fig. 4.7: Diagram of the computation methodology

4.2.1 Using Python scripts for data processing

The data used for the computation of the tilted GHI (Tables 4.1–4.6) were extracted through a Python script (Figure 4.8). This script extracts and processes the daily global horizontal irradiance (GHI) and direct normal irradiance (DNI) data for the specified coordinates, using the NASA POWER API. The data are then aggregated at monthly level, computing the monthly mean for GHI and DNI and determining the number of days in each month. The results are saved in a CSV file.

Table 4.1: Input data for Lake Bicaz for the tilted GHI computation

Month	**No. of days**	**DNI**	**GHI**
Longitude: 26.112°; Latitude: 46.949°; Tilt: 18°			
January	31	3.0	1.57
February	29	2.73	2.27
March	31	3.66	3.53
April	30	6.55	5.79
May	31	3.32	4.93
June	30	4.16	5.95
July	31	5.59	6.13
August	31	6.88	5.97
September	30	5.81	4.46
October	31	2.34	2.28
November	30	2.37	1.5
December	31	1.1	0.74

Table 4.2: Input data for Lake Colibiţa for the tilted GHI computation

Month	**No. of days**	**DNI**	**GHI**
Longitude: 24.898°; Latitude: 47.169°; Tilt: 18°			
January	31	2.82	1.44
February	29	2.4	1.82
March	31	3.24	3.14
April	30	6.65	5.57
May	31	2.98	4.51
June	30	2.88	5.7
July	31	4.16	5.27
August	31	6.25	5.73
September	30	5.16	4.2
October	31	1.87	1.99
November	30	2.64	1.49
December	31	1.97	1.2

Table 4.3: Input data for Lake Goleşti for the tilted GHI computation

Month	**No. of days**	**DNI**	**GHI**
Longitude: 24.98°; Latitude: 44.816°; Tilt: 18°			
January	31	3.75	1.92
February	29	3.56	2.55
March	31	3.56	3.43
April	30	6.33	5.86
May	31	4.28	5.63
June	30	4.55	5.99
July	31	6.8	6.47
August	31	5.94	5.8
September	30	5.54	4.74
October	31	2.93	2.67
November	30	2.29	1.56
December	31	0.78	0.74

Table 4.4: Input data for Lake Oaşa for the tilted GHI computation

Month	**No. of days**	**DNI**	**GHI**
Longitude: 23.62°; Latitude: 45.583°; Tilt: 18°			
January	31	3.18	1.67
February	29	2.88	2.13
March	31	3.37	3.24
April	30	6.2	5.62
May	31	3.43	5.1
June	30	3.42	5.15
July	31	5.45	5.81
August	31	5.6	5.56
September	30	4.95	4.31
October	31	2.57	2.38
November	30	2.42	1.52
December	31	1.64	1.6

Table 4.5: Input data for Lake Vidra for the tilted GHI computation

Month	**No. of days**	**DNI**	**GHI**
Longitude: 23.715909°; Latitude: 45.427412°; Tilt: 18°			
January	31	3.18	1.67
February	29	2.88	2.13
March	31	3.37	3.24
April	30	6.2	5.62
May	31	3.43	5.1
June	30	3.42	5.15
July	31	5.45	5.81
August	31	5.6	5.56
September	30	4.95	4.31
October	31	2.57	2.38
November	30	2.42	1.52
December	31	1.64	1.6

Table 4.6: Input data for Lake Vidraru for the tilted GHI computation

Month	**No. of days**	**DNI**	**GHI**
Longitude: 24.62936°; Latitude: 45.375287°; Tilt: 18°			
January	31	3.15	1.71
February	29	2.87	2.25
March	31	3.34	3.36
April	30	6.21	5.67
May	31	3.29	5.4
June	30	3.52	5.45
July	31	5.16	5.88
August	31	5.9	5.69
September	30	5.18	4.34
October	31	2.56	2.43
November	30	2.56	1.59
December	31	1.56	1.1

```python

# Setează coordonatele locației pentru care dorești datele
latitude = "45.248407"
longitude = "25.736816"
tilt = 18  # Valoare constantă pentru tilt

# Construiește parametrii pentru request
params = {
    "parameters": "ALLSKY_SFC_SW_DWN,ALLSKY_SFC_SW_DNI",
    "community": "RE",
    "longitude": longitude,
    "latitude": latitude,
    "format": "JSON",
    "start": "20200101",
    "end": "20201231",
    "tempAverage": "DAILY",
    "time": "24"
}

# URL-ul API-ului NASA POWER
url = "https://power.larc.nasa.gov/api/temporal/daily/point"

# Face request-ul
response = requests.get(url, params=params)

# Verifică dacă request-ul a fost cu succes
if response.status_code == 200:
    data = response.json()

    # Extrage datele pentru GHI și DNI și le pune într-o listă de dicționare
    records = []
    ghi_data = data['properties']['parameter']['ALLSKY_SFC_SW_DWN']
    dni_data = data['properties']['parameter']['ALLSKY_SFC_SW_DNI']
    for date_str in ghi_data:
        readable_date = datetime.strptime(date_str, "%Y%m%d")
        dni_value = dni_data.get(date_str, 'N/A')
        records.append({
            'Date': readable_date,
            'Longitude': longitude,
            'Latitude': latitude,
            'Tilt': tilt,
            'DNI': dni_value,
            'GHI': ghi_data[date_str]
        })

    # Crează un DataFrame din lista de dicționare
    df = pd.DataFrame(records)

    # Conversia coloanei 'Date' la tipul datetime și adăugarea unei coloane pentru lună și an
    df['Date'] = pd.to_datetime(df['Date'])
    df['YearMonth'] = df['Date'].dt.to_period('M')

    # Grupare pe lună și calcul medie pentru GHI și DNI
    monthly_avg = df.groupby('YearMonth').agg({'DNI': 'mean', 'GHI': 'mean'}).reset_index()

    # Calcularea numărului de zile din fiecare lună
    monthly_days = df.groupby('YearMonth').size().reset_index(name='Days')

    # Combină medii cu numărul de zile
    monthly_data = pd.merge(monthly_avg, monthly_days, on='YearMonth')
    # Ajustează numărul de zecimale pentru DNI și GHI la 4
    monthly_data['DNI'] = monthly_data['DNI'].round(2)
    monthly_data['GHI'] = monthly_data['GHI'].round(2)

    # Adaugă coloanele constante
    monthly_data['Longitude'] = float(longitude)
    monthly_data['Latitude'] = float(latitude)
    monthly_data['Tilt'] = tilt

    # Conversia coloanei 'YearMonth' înapoi la string pentru a ușura citirea și eliminarea coloanei YearMonth
    monthly_data = monthly_data[['Days', 'Longitude', 'Latitude', 'Tilt', 'DNI', 'GHI']]

    # Numele fișierului CSV unde vor fi salvate datele lunare
    csv_file_path = '/Users/panaitaureianandrei/Desktop/LicentaV1/ImportDniGhi/BarajulPaltinu.csv'


    # Salvarea datelor calculate într-un nou fișier CSV
    monthly_data.to_csv(csv_file_path, index=False)
```

Fig. 4.8: Python script for extracting and processing the daily DNI and GHI data (Annex 1)

4.2.2 Computation of the global horizontal irradiance on tilted surfaces (Annex 2)

```python
hsc = 1.353  # Solar constant value

def calculate_irradiance(df):
    results = []
    for index, row in df.iterrows():
        n = row['Days']
        latitude = row['Latitude']
        longitude = row['Longitude']
        tilt = row['Tilt']
        dni = row['DNI']
        ghi = row['GHI']
        delta = 23.45 * math.sin(deg_to_rad(360 * (284 + n) / 365))
        rb = (math.sin(deg_to_rad(latitude - tilt)) * math.sin(deg_to_rad(delta)) +
              math.cos(deg_to_rad(latitude - tilt)) * math.cos(deg_to_rad(delta)) * math.cos(deg_to_rad(longitude))) / (
                     math.sin(deg_to_rad(latitude)) * math.sin(deg_to_rad(delta)) +
                     math.cos(deg_to_rad(latitude)) * math.cos(deg_to_rad(longitude)) * math.cos(deg_to_rad(delta)))
        rd = (1 + math.cos(deg_to_rad(tilt))) / 2
        rr = (1 - math.cos(deg_to_rad(tilt))) / 2
        hs = rad_to_rad(math.acos(-math.tan(deg_to_rad(latitude)) * math.tan(deg_to_rad(delta))))
        ho = ((hsc / pi) * 24) * (1 + 0.033 * math.cos(deg_to_rad(360 * n) / 365)) * (
                    (math.cos(deg_to_rad(latitude)) * math.cos(deg_to_rad(delta)) * math.sin(deg_to_rad(hs))) +
                    ((((2 * pi) / 360) * hs) * math.sin(deg_to_rad(latitude)) * math.sin(deg_to_rad(delta))))
        kt = dni / ho
        hd = ghi * ((0.775 + (0.00653 * (hs - 90))) - (0.505 + (0.00455 * (hs - 90))) * (math.cos(deg_to_rad(115 * kt - 103))))
        hb = (ghi - hd)
        roh = 0.5
        hr = ghi * roh
        ht = hr * rr + hb * rb + hd * rd
        results.append(ht)
    return results

mesi = ['January', 'February', 'March', 'April', 'May', 'June', 'July', 'August', 'September', 'October', 'November', 'December']

def calculate_monthly_irradiance(lake_name, df):
    monthly_irradiance = {month: [] for month in mesi}
    for tilt_angle in range(0, 46):  # Limit tilt angles to 0 to 45 degrees
        df['Tilt'] = tilt_angle
        irradiance = calculate_irradiance(df)
        for i, month in enumerate(mesi):
            monthly_irradiance[month].append(irradiance[i])
    return monthly_irradiance

def find_max_irradiance(monthly_irradiance):
    max_irradiance = {}
    for month in mesi:
        max_value = max(monthly_irradiance[month])
        max_angle = monthly_irradiance[month].index(max_value)
        max_irradiance[month] = (max_angle, max_value)
    return max_irradiance
```

Fig. 4.9: Python script for the tilted GHI computation

```python
def plot_irradiance(lake_name, monthly_irradiance, max_irradiance):
    plt.figure(figsize=(15, 10))
    for i, month in enumerate(mesi):
        plt.subplot(4, 3, i + 1)
        plt.plot(range(0, 46), monthly_irradiance[month])  # Plot for tilt angles 0 to 45 degrees
        plt.xlabel('Tilt angles (degrees)')
        plt.ylabel('GHI tilted (kWh/m2)')
        plt.title(f'{month}')
        max_angle, max_value = max_irradiance[month]
        plt.axvline(x=max_angle, color='r', linestyle='--')
        plt.text(max_angle, max_value, f'{max_value:.2f}', color='red')
    plt.tight_layout()
    plt.suptitle(f'Tilted Solar Irradiance for {lake_name}')
    plt.subplots_adjust(top=0.95)
    plt.show()

def analyze_lake(lake_name):
    df = data_frames[lake_name]
    monthly_irradiance = calculate_monthly_irradiance(lake_name, df)
    max_irradiance = find_max_irradiance(monthly_irradiance)
    plot_irradiance(lake_name, monthly_irradiance, max_irradiance)

    # Save results to CSV
    results = []
    for month in mesi:
        angle, value = max_irradiance[month]
        results.append([lake_name, month, angle, round(value, 2)])
        print(f'The maximum value of tilted solar irradiance on the {lake_name} for the month {month} happens at a tilt angle {angle} degrees and the corresponding solar irradiance is {round(value, 2)}')

    # Define the CSV file path
    csv_file = f'/Users/panaitaureianandrei/Desktop/{lake_name}_solar_irradiance.csv'

    # Write the results to the CSV file
    with open(csv_file, mode='w', newline='') as file:
        writer = csv.writer(file)
        writer.writerow(['Lake', 'Month', 'Tilt Angle (degrees)', 'Solar Irradiance (kWh/m2)'])
        writer.writerows(results)

    print(f'Results have been saved to {csv_file}')

# Call the function for the desired lake
analyze_lake('Vidraru')
```

Fig. 4.10: Python script for the tilted GHI computation

4.3 Detailed Computation Method for the Tilted Global Horizontal Irradiance

In this study, DNI, GHI, the tilt angle and a Python script were used to obtain the tilted GHI, since this allows a much more accurate quantification of the monthly solar potential.

The tilted GHI (H_T) was computed using equations (4.1)–(4.11). Six parameters were used in this equation, namely H_b (beam irradiation), H_d (diffuse irradiation), H_r (reflected irradiation), R_b (tilt factor for beam irradiation), R_d (tilt factor for diffuse irradiation) and R_r (tilt factor for reflected irradiation), and they were computed using the Python programming language. The input file, containing parameters such as the days (n, the day of the month), the latitude (φ, degrees), omega (ω, degrees relative to time), the tilt angle (s, in degrees relative to the site latitude ±10°), the daily radiation (kWh relative to the month) and H (GHI, kWh), was used to compute the aforementioned terms. These terms were then used to compute the tilted GHI using equation (4.11).

The algorithm presented in Figures 4.9 and 4.10 was implemented in Python in order to convert GHI into tilted GHI. This tilted GHI is subsequently used to compute the solar potential assessment of the selected study area. In this algorithm, an input file is used to enter the values of the various parameters. The value of the declination (δ) was computed using equation (4.1), based on the number of days in a year.

4.3.1 Computed parameters and equations used

The declination:

$$\delta = 23.45 \left[\sin \frac{360}{365} (284 + n) \right] \tag{4.1}$$

The next step after the declination was the computation of the sunset hour angle (h_s, equation (4.2)), using the declination angle and the latitude of the site.

$$h_s = \cos^{-1} \left[-\tan(\varphi) \tan(\delta) \right] \tag{4.2}$$

The value of the extraterrestrial solar irradiance is a solar constant, valid in space, where no disturbing elements exist. The extraterrestrial solar irradiance value used in this study is H_{sc} = 1353 W/m^2. The daily extraterrestrial solar irradiation (H_0', equation (4.3)) was computed in order to estimate the tilted GHI.

$$H_0' = H_{sc} \left[1 + 0.033 \left(\frac{360n}{365} \right) \right] \left[\cos(\varphi) \cos(\delta) \sin(h_s) + \frac{2\pi h_s}{360} \sin(\varphi) \sin(\delta) \right] \tag{4.3}$$

The clearness index (K_T, equation (4.4)) was computed using the solar constant in space and at the study location.

$$K_T = \frac{H}{H_0'} \tag{4.4}$$

The irradiation that is scattered by dust particles and aerosols is called diffuse irradiation (Muneer et al. 2002). This diffuse irradiation (H_d, equation (4.5)) was computed using h_s and K_T.

$$H_d = [0.775 + 0.00653 (h_s - 90) - \{0.0505 + 0.0045 (h_s - 90)\} \cos (115 K_T - 103)] \tag{4.5}$$

The irradiation that falls directly on the Earth's surface without changing its trajectory is called beam irradiation. The GHI (H, equation (4.6)) is the sum of the beam irradiation (H_b) and the diffuse irradiation (H_d).

$$H_b = H - H_d \tag{4.6}$$

The beam irradiation was computed using this relation. The tilt factor for beam irradiation (R_b, equation (4.7)), for diffuse irradiation (R_d, equation (4.8)) and for reflected irradiation (R_r, equation (4.9)) were computed using the equations presented below, based on the latitude (φ), the tilt angle (s), omega (ω) and the declination (δ). These computed parameters were used to determine the tilted GHI using equation (4.11).

$$R_b = \frac{\sin(\varphi - s)\sin(\delta) + \cos(\varphi - s)\cos(\delta)\cos(\omega)}{\sin(\varphi)\sin(\delta) + \cos(\varphi)\cos(\delta)\cos(\omega)} \tag{4.7}$$

$$R_d = \frac{1 + \cos(s)}{2} \tag{4.8}$$

$$R_r = \frac{1 - \cos(s)}{2} \tag{4.9}$$

$$H_r = (H_b + H_d)\,\rho_g \tag{4.10}$$

where ρ_g is the ground reflection coefficient (0.5).

$$H_t = H_b R_b + H_d R_d + H_r R_r \tag{4.11}$$

4.4 Simulation and Computation Results – Case I (45° tilt)

The Case I tables (4.7–4.13) and the Case II tables (4.14–4.20) contain information on the computed solar irradiation (tilted GHI) of the studied lakes for the 12 months of the year.

In both cases the computations use the same tilt angle for all lakes (45 and 10 degrees respectively), which ensures the comparability of the data.

The Solar Irradiation column (kWh/m^2) contains the computed monthly values of the tilted global horizontal irradiance needed to identify the energy potential and the optimal location for placing FPV. The values are expressed in kilowatt-hours per square metre (kWh/m^2) and vary depending on the location and the period of the year.

The first case (I), in which we analyse the potential at a tilt of 45 degrees.

Figures 4.11 and 4.12 present the variations of the maximum solar irradiation for all six lakes over a calendar year at the 45-degree tilt angle.

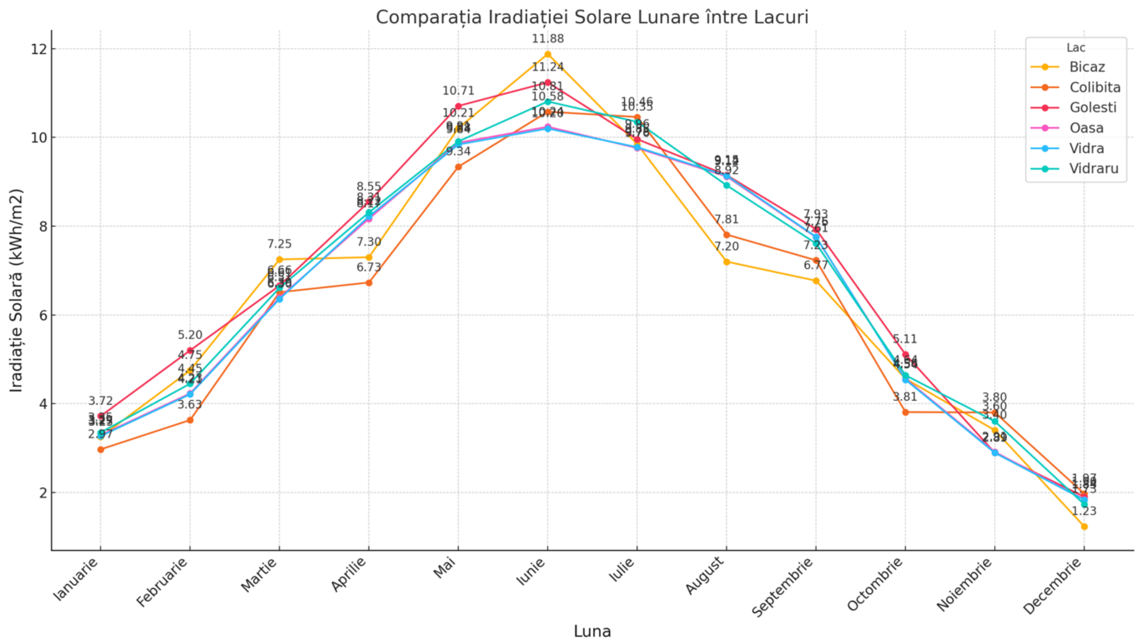

Fig. 4.11: Monthly values of the tilted GHI solar irradiation

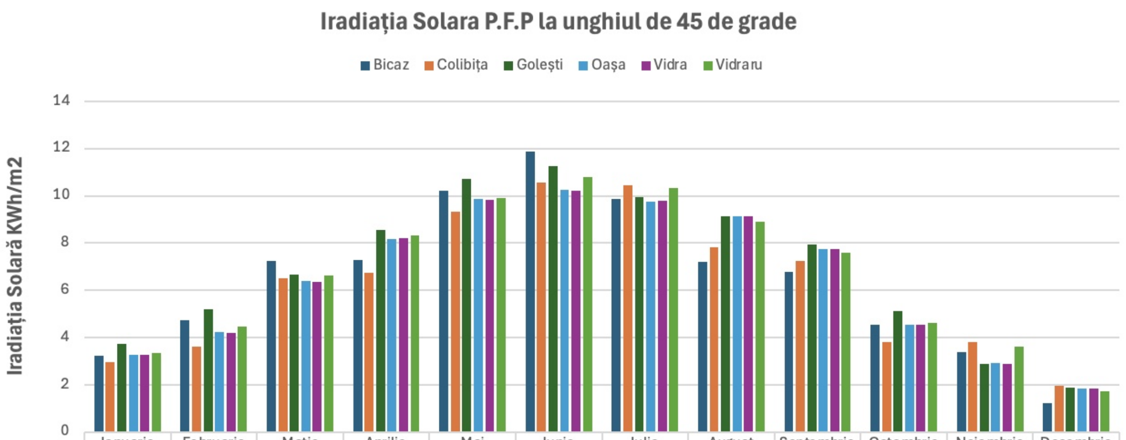

	Ianuarie	Februarie	Matie	Aprilie	Mai	Iunie	Iulie	August	Septembrie	Octombrie	Noiembrie	Decembrie
Bicaz	3,25	4,75	7,25	7,3	10,21	11,88	9,85	7,2	6,77	4,56	3,4	1,23
Colibița	2,97	3,63	6,51	6,73	9,34	10,58	10,46	7,81	7,23	3,81	3,8	1,97
Golești	3,72	5,2	6,66	8,55	10,71	11,24	9,96	9,15	7,93	5,11	2,89	1,9
Oașa	3,29	4,23	6,39	8,17	9,88	10,24	9,76	9,12	7,75	4,56	2,91	1,84
Vidra	3,27	4,21	6,36	8,22	9,84	10,2	9,78	9,14	7,76	4,54	2,89	1,83
Vidraru	3,35	4,45	6,61	8,31	9,91	10,81	10,35	8,92	7,61	4,64	3,6	1,73

Lunile Anului

Fig. 4.12: Monthly values of the tilted GHI solar irradiation

The seasonal variations increase significantly from January to June, reaching a peak in midsummer (July), then decrease gradually until December. This pattern is consistent across all locations.

Although the general trends are similar, the magnitude of the solar irradiation varies with the location. For example, Bicaz can have higher irradiation values compared with other locations, indicating a potential advantage for solar energy projects in that area.

The May–August months have the highest solar irradiation, making them the most suitable for solar energy capture.

4.4.1 (I) Tables of the monthly tilted GHI values for the studied lakes

Table 4.7: Resulting monthly tilted GHI values for Lake Bicaz

Month	Solar irradiation (kWh/m^2)
Tilt angle: 45°	
January	3.25
February	4.75
March	7.25
April	7.3
May	10.21
June	11.88
July	9.85
August	7.2
September	6.77
October	4.56
November	3.4
December	1.23

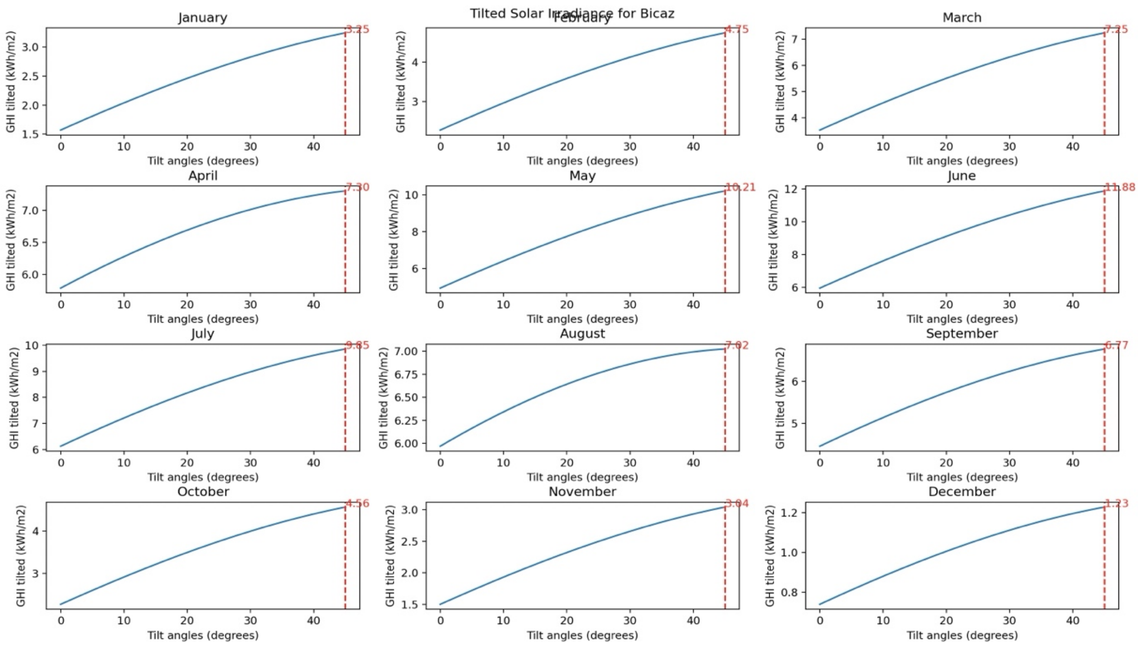

Fig. 4.13: Graphical monthly tilted GHI values for Lake Bicaz

Table 4.8: Resulting monthly tilted GHI values for Lake Colibiţa

Month	**Solar irradiation (kWh/m^2)**
Tilt angle: 45°	
January	2.97
February	3.63
March	6.51
April	6.73
May	9.34
June	10.58
July	10.46
August	7.81
September	7.23
October	3.81
November	3.8
December	1.97

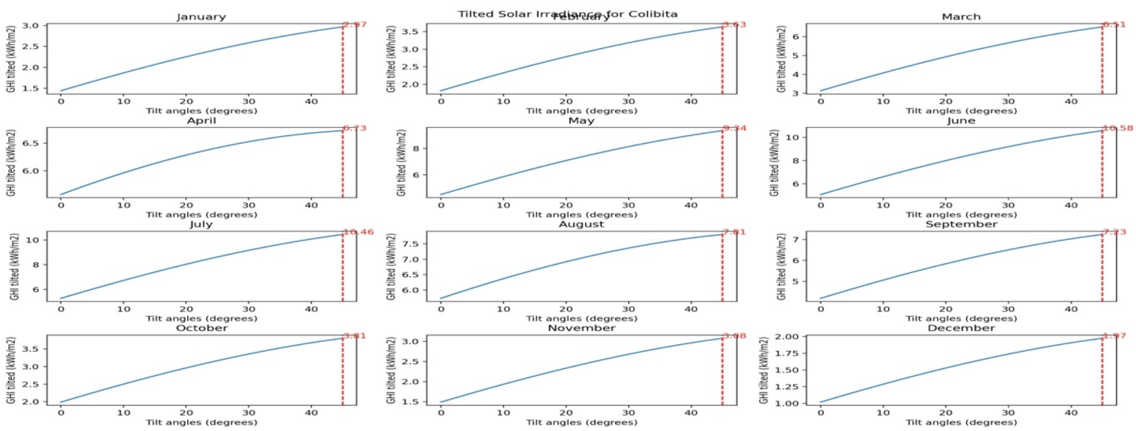

Fig. 4.14: Graphical monthly tilted GHI values for Lake Colibiţa

Table 4.9: Resulting monthly tilted GHI values for Lake Goleşti

Month	**Solar irradiation (kWh/m^2)**
Tilt angle: 45°	
January	3.72
February	5.2
March	6.66
April	8.55
May	10.71
June	11.24
July	9.96
August	9.15
September	7.93
October	5.11
November	2.89
December	1.9

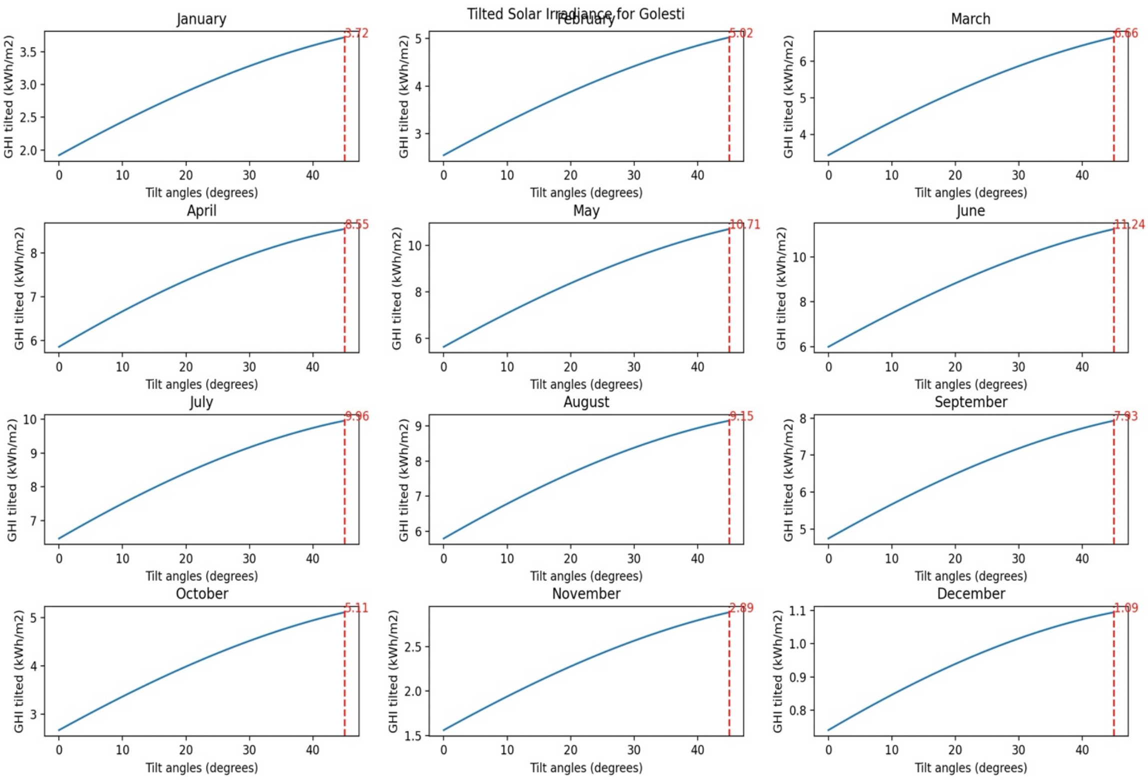

Fig. 4.15: Graphical monthly tilted GHI values for Lake Goleşti

Table 4.10: Resulting monthly tilted GHI values for Lake Oaşa

Month	**Solar irradiation (kWh/m^2)**
Tilt angle: 45°	
January	3.29
February	4.23
March	6.39
April	8.17
May	9.88
June	10.24
July	9.76
August	9.12
September	7.75
October	4.56
November	2.91
December	1.84

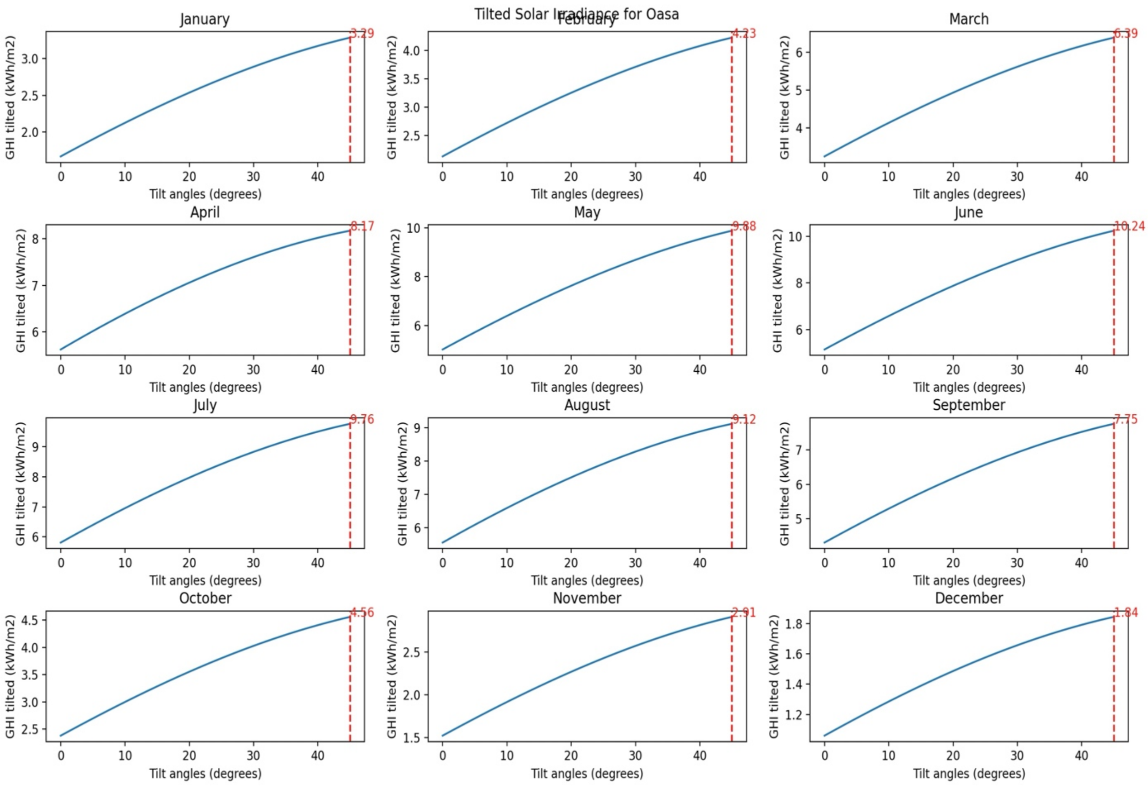

Fig. 4.16: Graphical monthly tilted GHI values for Lake Oaşa

Table 4.11: Resulting monthly tilted GHI values for Lake Vidra

Month	**Solar irradiation (kWh/m^2)**
Tilt angle: 45°	
January	3.27
February	4.21
March	6.36
April	8.22
May	9.84
June	10.2
July	9.78
August	9.14
September	7.76
October	4.54
November	2.89
December	1.83

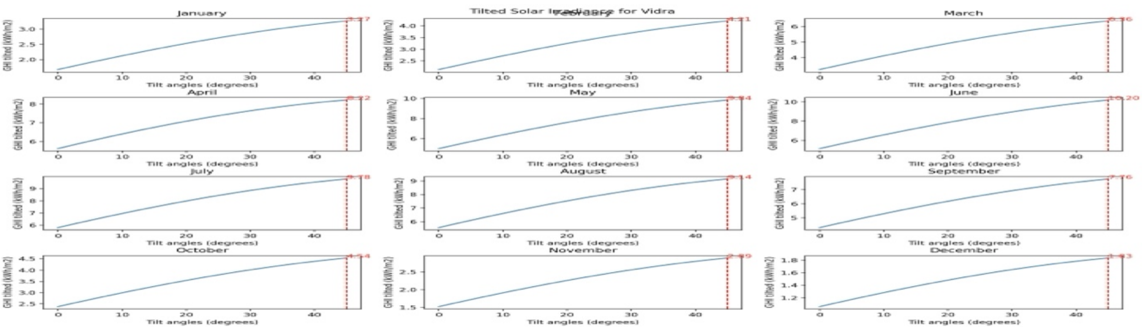

Fig. 4.17: Graphical monthly tilted GHI values for Lake Vidra

Table 4.12: Resulting monthly tilted GHI values for Lake Vidraru

Month	**Solar irradiation (kWh/m^2)**
Tilt angle: 45°	
January	3.35
February	4.45
March	6.61
April	8.31
May	9.91
June	10.81
July	10.35
August	8.92
September	7.61
October	4.64
November	3.6
December	1.73

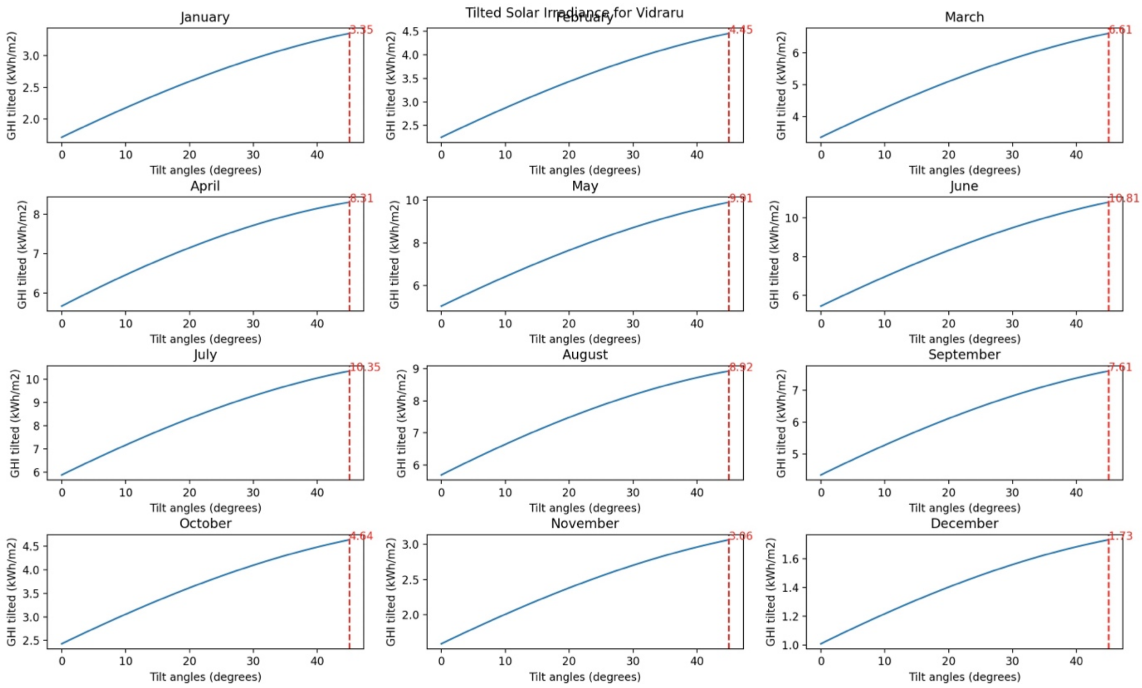

Fig. 4.18: Graphical monthly tilted GHI values for Lake Vidraru

4.5 (I) Analysis of the Optimal Locations for Solar Panels

In order to determine the optimal locations for installing solar panels, several key criteria based on the statistical analysis of the solar irradiation must be taken into consideration (Table 4.13):

1. **Mean solar irradiation:** locations with higher mean solar irradiation values are preferred, since they will generate more energy over the year.
2. **Solar irradiation variability:** locations with a lower standard deviation and a smaller range are preferable, since they offer a more constant energy production, reducing the need for energy storage during periods of low irradiation.
3. **Minimum and maximum values:** high maximum values are an advantage, but it is important that the minimum values are not very low, in order to ensure a constant production.

Table 4.13: Centralised statistical values

Location	N	Mean kWh/m^2	Std. dev.	Min kWh/m^2	P25 kWh/m^2	Median (P50) kWh/m^2	P75 kWh/m^2	Max kWh/m^2	Range
Bicaz	12	6.47	3.17	1.23	4.27	6.99	7.94	11.88	10.65
Colibiţa	12	6.24	2.98	1.97	3.76	6.62	8.19	10.58	8.61
Goleşti	12	6.92	3.15	1.9	4.76	7.3	9.35	11.24	9.34
Oaşa	12	6.51	3.03	1.84	4	7.07	9.28	10.24	8.4
Vidra	12	6.5	3.04	1.83	3.98	7.06	9.3	10.2	8.37
Vidraru	12	6.69	3.07	1.73	4.24	7.11	9.17	10.81	9.08

4.5.1 (I) Description of the statistical table data and the statistical equations used

The columns of the statistical table (Figure 4.19):

1. **Location:** the name of the location where the solar irradiation values were determined (e.g. Bicaz, Colibiţa, Goleşti etc.).

2. **Number of values:** the total number of records (months) for each location. Computation: the number of months for which the solar irradiation values were computed. Example: for each location we have 12 computed values, one for each month of the year.

3. **Mean:** the arithmetic mean of the solar irradiation values for each location (equation (4.12)). Computation: the sum of all solar irradiation values for a location divided by the total number of records (months).

$$\text{Mean} = \frac{\sum \text{GHI}}{\text{Number of values}} \tag{4.12}$$

$$\begin{aligned}\text{Ex. Bicaz : Mean} = \tfrac{1}{12}\,&(3.25 + 4.75 + 7.25 + 7.30 + 10.21 + 11.88\\ &+ 9.85 + 7.20 + 6.77 + 4.56 + 3.40 + 1.23) = 6.47\ \text{kWh/m}^2\end{aligned}$$

4. **Standard deviation:** the measure of the variability or dispersion of the solar irradiation values relative to the annual mean. Computation: the square root of the variance, where the variance is the mean of the squared deviations from the mean of the values (equation (4.13)).

$$\sigma = \sqrt{\frac{\sum (x_i - \text{Mean})^2}{n}} \tag{4.13}$$

Example: the standard deviation for Bicaz is computed on the basis of the differences of each value from the mean of 6.47.

5. **Minimum (Min):** the smallest solar irradiation value computed for each location. Computation: the minimum value in the data set for a location. Example: for Bicaz, the minimum value is 1.23 kWh/m^2.

6. **25th percentile:** the value below which 25% of the solar irradiation values lie. Computation: the values are sorted in ascending order and the value separating the first 25% of the data is identified. Example: the 25th percentile for Bicaz is computed on the basis of the values sorted in ascending order.

7. **Median (50th percentile):** the middle value of the data set, which divides the data into two equal parts. Computation: the values are sorted in ascending order and the middle value is identified. Example: the median for Bicaz is computed on the basis of the values sorted in ascending order.

8. **75th percentile:** the value below which 75% of the solar irradiation values lie. Computation: the values are sorted in ascending order and the value separating the first 75% of the data is identified. Example: the 75th percentile for Bicaz is computed on the basis of the values sorted in ascending order.
9. **Maximum:** the largest solar irradiation value recorded for each location. Computation: the maximum value in the data set for a location. Example: for Bicaz, the maximum value is 11.88 kWh/m^2.
10. **Range:** the difference between the maximum and the minimum value for each location. Computation: Range = Max − Min. Example: for Bicaz, the range is 11.88 − 1.23 = 10.65 kWh/m^2.

Complete example for the Bicaz location:

1. Number of values: 12 (one for each month of the year)
2. Mean
3. Standard deviation: computed on the basis of the deviation of each value from the mean of 6.47
4. Minimum: 1.23 kWh/m^2
5. 25th percentile: approximately 4.27 kWh/m^2 (computed on the basis of the sorted values)
6. Median: approximately 6.99 kWh/m^2 (computed on the basis of the sorted values)
7. 75th percentile: approximately 7.94 kWh/m^2 (computed on the basis of the sorted values)
8. Maximum: 11.88 kWh/m^2
9. Range: 11.88 − 1.23 = 10.65 kWh/m^2

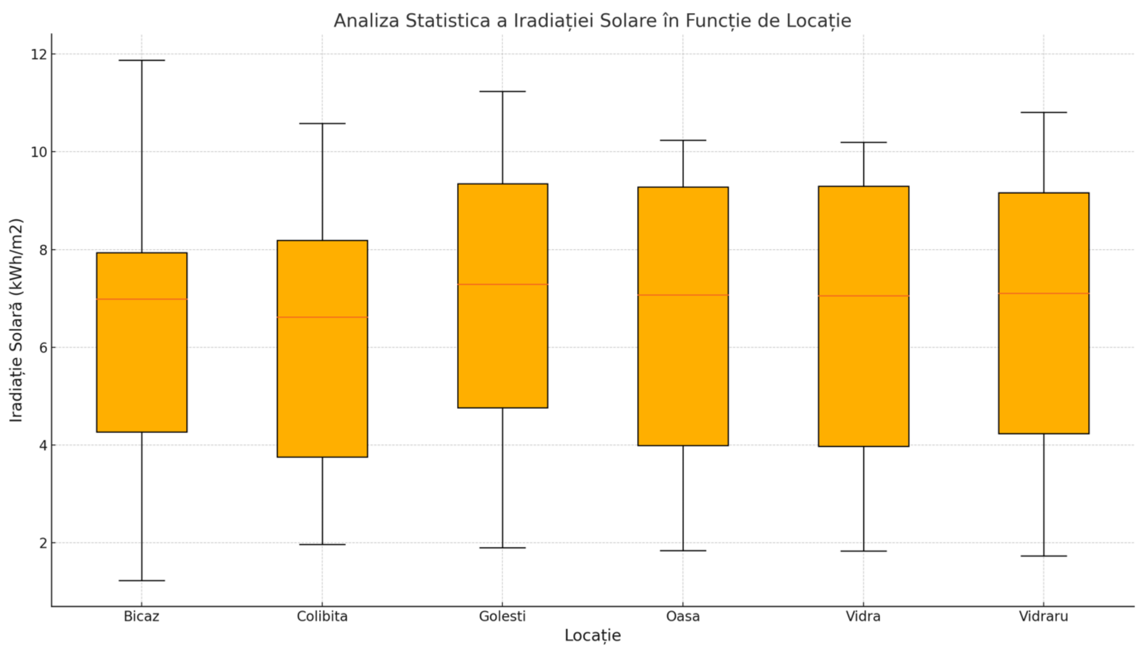

Fig. 4.19: Boxplot chart

4.6 (I) Description of the Statistical Chart: Boxplot of the Solar Irradiation

The boxplot chart presented illustrates the distribution of the solar irradiation values for each location included in the analysis. This chart is useful for visualising the variability of the data, as well as for identifying possible extreme values (outliers).

4.6.1 (I) Elements of the boxplot chart

1. **The box:**
   - *Median line:* the horizontal line inside each box represents the median of the solar irradiation values for that location. This is the value that divides the data set into two equal parts.
   - *Box edges (Inter-Quartile Range, IQR):* the upper and lower edges of the box represent the 25th percentile (Q1) and the 75th percentile (Q3). They indicate the interval containing the central 50% of the data values.
2. **The whiskers:** the whiskers extend from the box edges to the smallest and largest values in the data set that are not considered outliers. These values are determined as lying at most 1.5 times the IQR distance from Q1 and Q3.
3. **Extreme values (outliers):** the points located outside the whiskers are considered extreme values (outliers). They represent solar irradiation values that are significantly higher or lower than the rest of the data set.

4.6.2 (I) Observations from the chart

1. **Solar irradiation variability:**
   - *Wide ranges:* locations such as Bicaz and Goleşti show wide ranges of solar irradiation values, indicating significant variability throughout the year.
   - *Different medians:* the median solar irradiation varies between locations, showing differences in the mean level of solar energy received. For example, Goleşti has a higher median compared with Colibiţa.
2. **Extreme values (outliers):**
   - *Bicaz:* shows some high extreme values, suggesting periods with solar irradiation much higher than the mean.
   - *Colibiţa:* has fewer extreme values, which indicates a more uniform distribution of the solar irradiation.
3. **Comparison of the locations:**
   - *Bicaz:* has the highest solar irradiation variability, with a range from 1.23 kWh/m^2 to 11.88 kWh/m^2.
   - *Colibiţa:* has the lowest variability, with a range from 1.97 kWh/m^2 to 10.58 kWh/m^2.
   - *Goleşti:* has the highest median and consistently high values, which makes it favourable for solar energy projects.

Conclusions:

- **Solar project planning:** locations with higher means and smaller ranges are more predictable and can be more advantageous for solar energy projects.
- **Risk analysis:** locations with high variability might require additional risk management strategies, such as energy storage for periods of low irradiation.

4.7 (I) Optimal Locations for FPV Placement

4.7.1 (I) Lake Goleşti

- **High mean:** 6.92 kWh/m^2, the highest of all analysed locations.
- **Moderate variability:** although the standard deviation and the range are relatively large, the maximum values are high, indicating a good potential for solar energy production.

4.7.2 (I) Lake Vidraru

- **High mean:** 6.69 kWh/m^2.
- **Moderate variability:** the minimum and maximum values are good, with a relatively large range, but with a high mean and constant production.

4.7.3 (I) Lake Oaşa

- **Moderate mean:** 6.51 kWh/m^2.
- **Low variability:** the range and the standard deviation are smaller, providing a more constant production.

Conclusions (I):

- Goleşti and Vidraru are the most suitable locations for installing solar panels owing to their high mean solar irradiation values, offering the potential for high electricity production.
- Oaşa is also a good location, offering a more constant production owing to the lower variability of the solar irradiation.
- Other locations, such as Bicaz, although they have high maximum values, show a higher variability, which may require additional energy storage solutions.

4.8 Simulation and Computation Results – Case II (10° tilt)

The second case (II), in which we analyse the potential at a tilt of 10 degrees.

Figures 4.20 and 4.21 present the variations of the maximum solar irradiation for all six lakes over a calendar year at the 10-degree tilt angle.

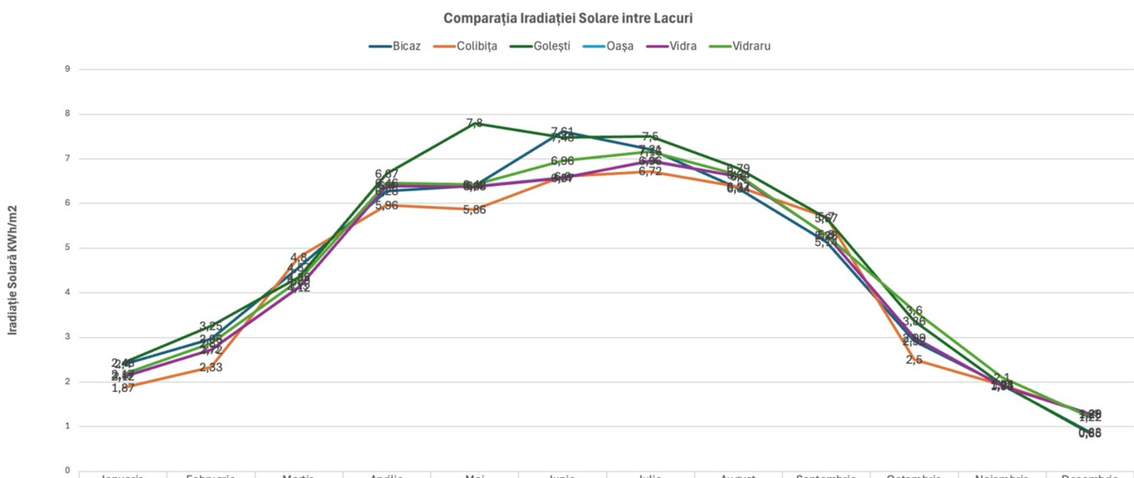

	Ianuarie	Februarie	Martie	Aprilie	Mai	Iunie	Iulie	August	Septembrie	Octombrie	Noiembrie	Decembrie
Bicaz	2,4	2,96	4,57	6,28	6,4	7,61	7,21	6,34	5,14	2,92	1,93	0,88
Colibița	1,87	2,33	4,8	5,96	5,86	6,6	6,72	6,37	5,7	2,5	1,93	1,29
Golești	2,43	3,25	4,35	6,67	7,8	7,48	7,5	6,79	5,67	3,36	1,94	0,85
Oașa	2,13	2,72	4,13	6,39	6,39	6,58	6,95	6,6	5,29	3	1,91	1,29
Vidra	2,12	2,72	4,12	6,4	6,38	6,57	6,96	6,6	5,3	2,99	1,91	1,28
Vidraru	2,17	2,87	4,28	6,46	6,42	6,96	7,16	6,64	5,28	3,6	2,1	1,22

Fig. 4.20: Monthly values of the tilted GHI solar irradiation

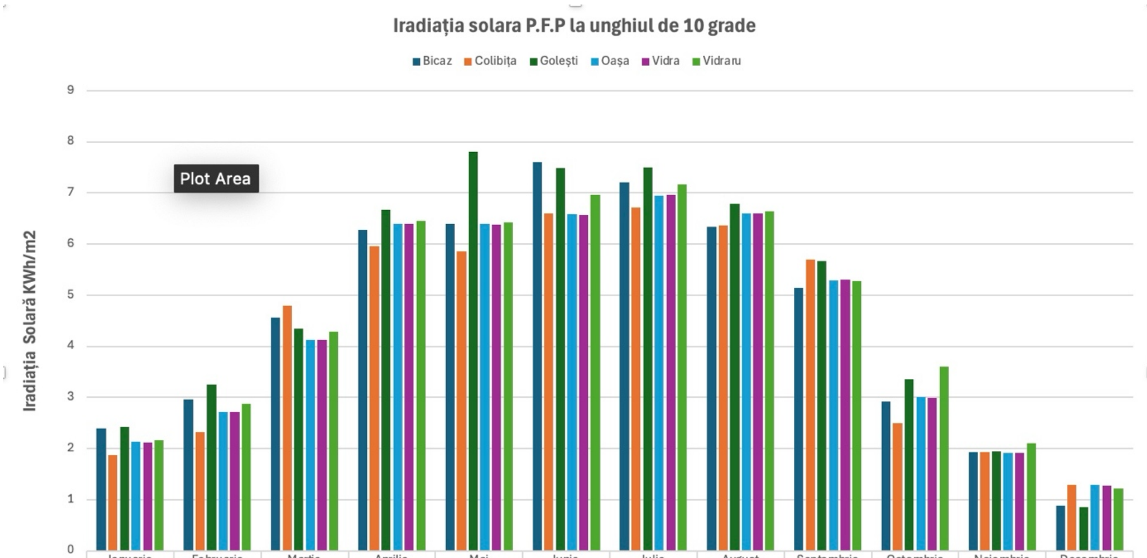

	Ianuarie	Februarie	Martie	Aprilie	Mai	Iunie	Iulie	August	Septembrie	Octombrie	Noiembrie	Decembrie
Bicaz	2,4	2,96	4,57	6,28	6,4	7,61	7,21	6,34	5,14	2,92	1,93	0,88
Colibița	1,87	2,33	4,8	5,96	5,86	6,6	6,72	6,37	5,7	2,5	1,93	1,29
Golești	2,43	3,25	4,35	6,67	7,8	7,48	7,5	6,79	5,67	3,36	1,94	0,85
Oașa	2,13	2,72	4,13	6,39	6,39	6,58	6,95	6,6	5,29	3	1,91	1,29
Vidra	2,12	2,72	4,12	6,4	6,38	6,57	6,96	6,6	5,3	2,99	1,91	1,28
Vidraru	2,17	2,87	4,28	6,46	6,42	6,96	7,16	6,64	5,28	3,6	2,1	1,22

Lunile Anului

Fig. 4.21: Monthly values of the tilted GHI solar irradiation

The seasonal variations increase significantly from January to June, reaching a peak at the end of May, then decrease gradually until December. This pattern is consistent across all locations.

Although the general trends are similar, the magnitude of the solar irradiation varies with the location. For example, Goleşti can have higher irradiation values compared with other locations, indicating a potential advantage for solar energy projects in that area.

The May–August months have the highest solar irradiation, making them the most suitable for solar energy capture.

4.8.1 (II) Tables of the monthly tilted GHI values for the studied lakes

Table 4.14: Resulting monthly tilted GHI values for Lake Bicaz

Month	Solar irradiation (kWh/m^2)
Tilt angle: 10°	
January	2.4
February	2.96
March	4.57
April	6.28
May	6.4
June	7.61
July	7.21
August	6.34
September	5.14
October	2.92
November	1.93
December	0.88

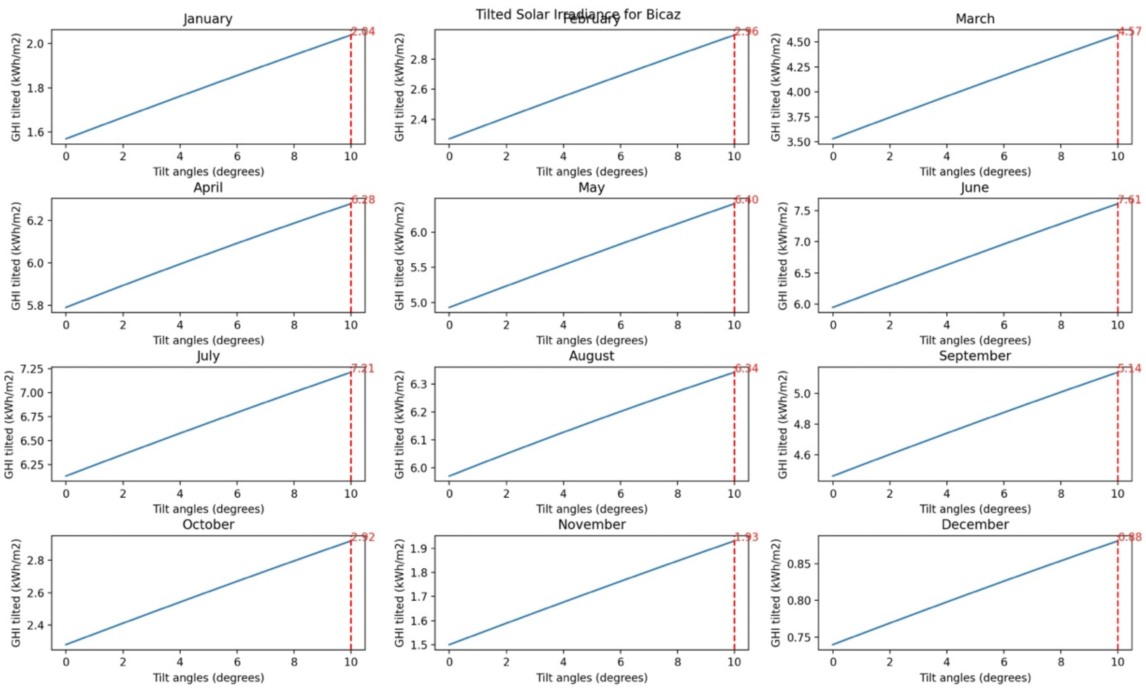

Fig. 4.22: Graphical monthly tilted GHI values for Lake Bicaz

Table 4.15: Resulting monthly tilted GHI values for Lake Colibiţa

Month	Solar irradiation (kWh/m^2)
Tilt angle: 10°	
January	1.87
February	2.33
March	4.8
April	5.96
May	5.86
June	6.6
July	6.72
August	6.37
September	5.7
October	2.5
November	1.93
December	1.29

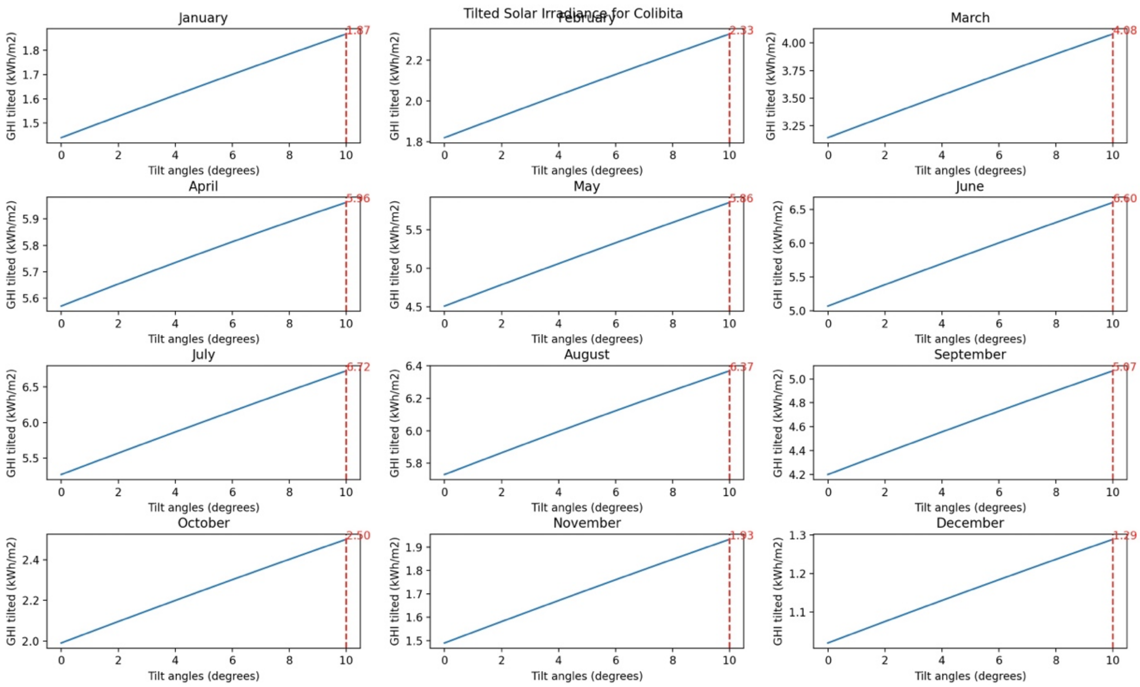

Fig. 4.23: Graphical monthly tilted GHI values for Lake Colibiţa

Table 4.16: Resulting monthly tilted GHI values for Lake Goleşti

Month	Solar irradiation (kWh/m^2)
Tilt angle: 10°	
January	2.43
February	3.25
March	4.35
April	6.67
May	7.8
June	7.48
July	7.5
August	6.79
September	5.67
October	3.36
November	1.94
December	0.85

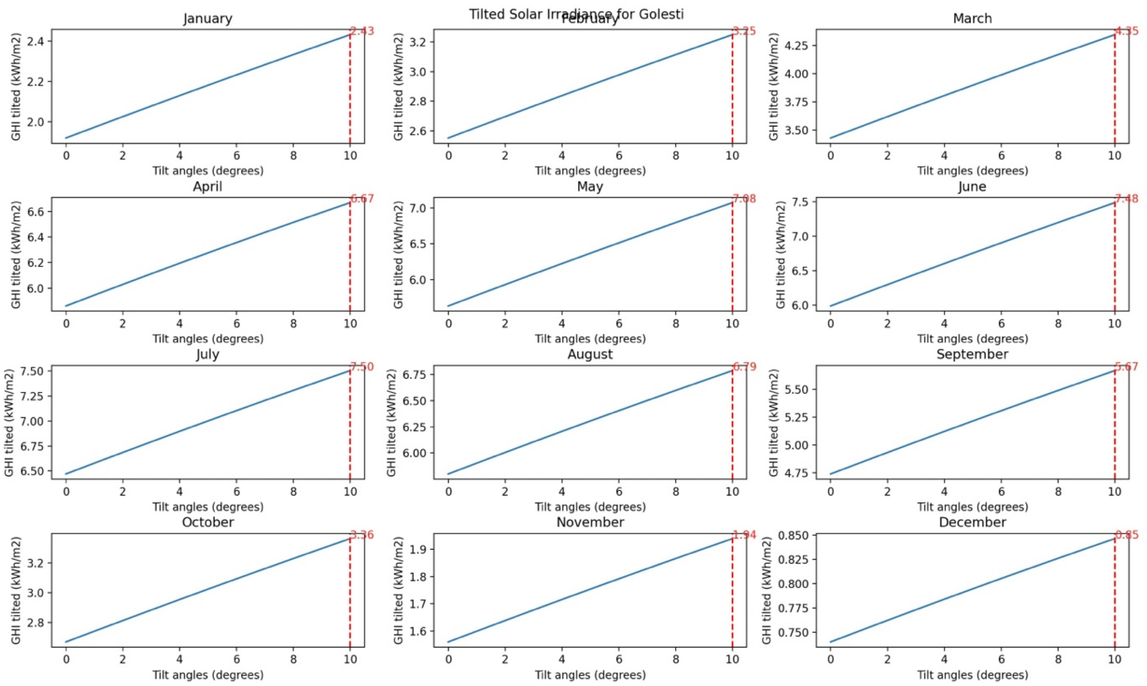

Fig. 4.24: Graphical monthly tilted GHI values for Lake Goleşti

Table 4.17: Resulting monthly tilted GHI values for Lake Oaşa

Month	Solar irradiation (kWh/m^2)
Tilt angle: 10°	
January	2.13
February	2.72
March	4.13
April	6.39
May	6.39
June	6.58
July	6.95
August	6.6
September	5.29
October	3
November	1.91
December	1.29

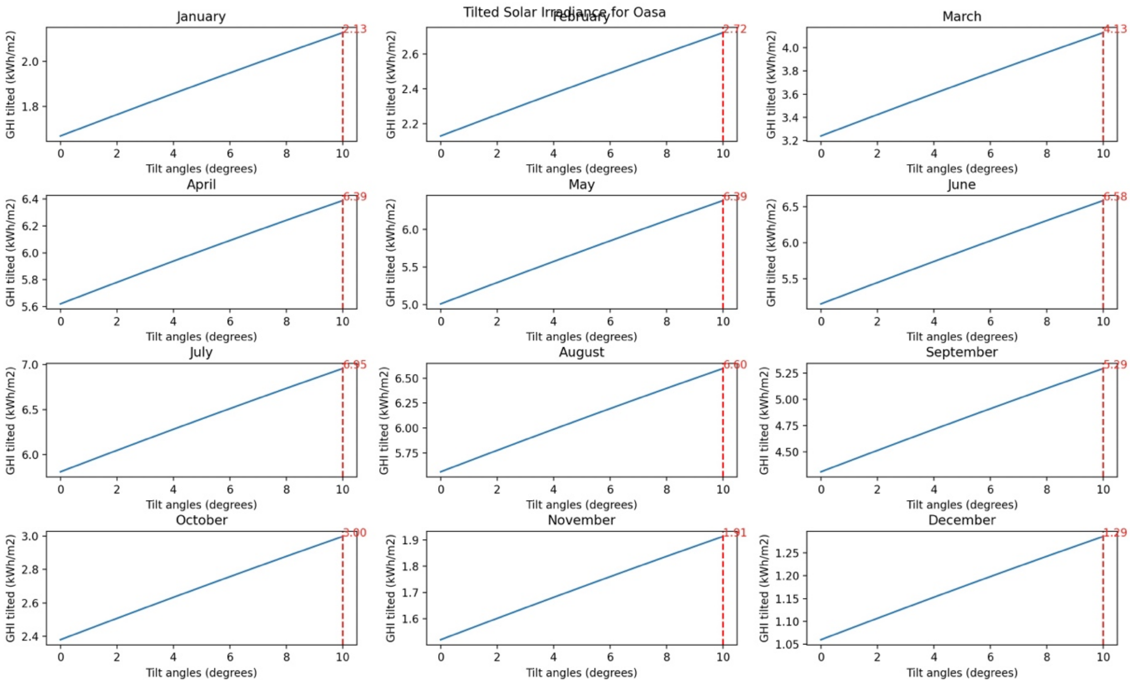

Fig. 4.25: Graphical monthly tilted GHI values for Lake Oaşa

Table 4.18: Resulting monthly tilted GHI values for Lake Vidra

Month	Solar irradiation (kWh/m^2)
Tilt angle: 10°	
January	2.12
February	2.72
March	4.12
April	6.4
May	6.38
June	6.57
July	6.96
August	6.6
September	5.3
October	2.99
November	1.91
December	1.28

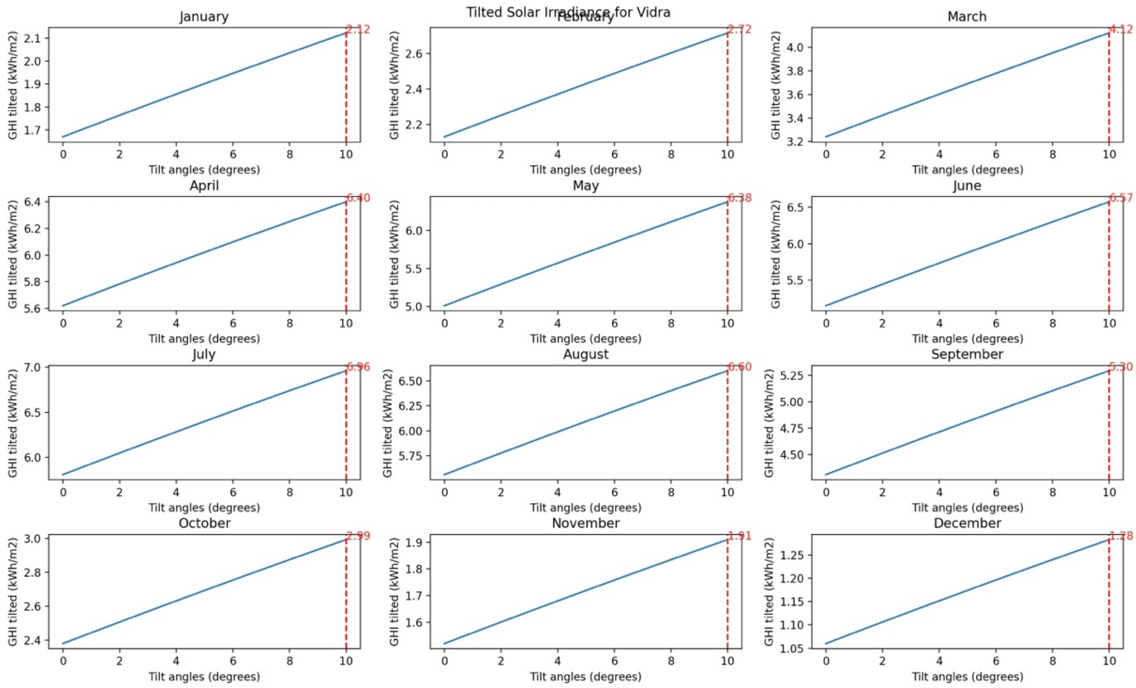

Fig. 4.26: Graphical monthly tilted GHI values for Lake Vidra

Table 4.19: Resulting monthly tilted GHI values for Lake Vidraru

Month	**Solar irradiation (kWh/m^2)**
Tilt angle: 10°	
January	2.17
February	2.87
March	4.28
April	6.46
May	6.42
June	6.96
July	7.16
August	6.64
September	5.28
October	3.6
November	2.1
December	1.22

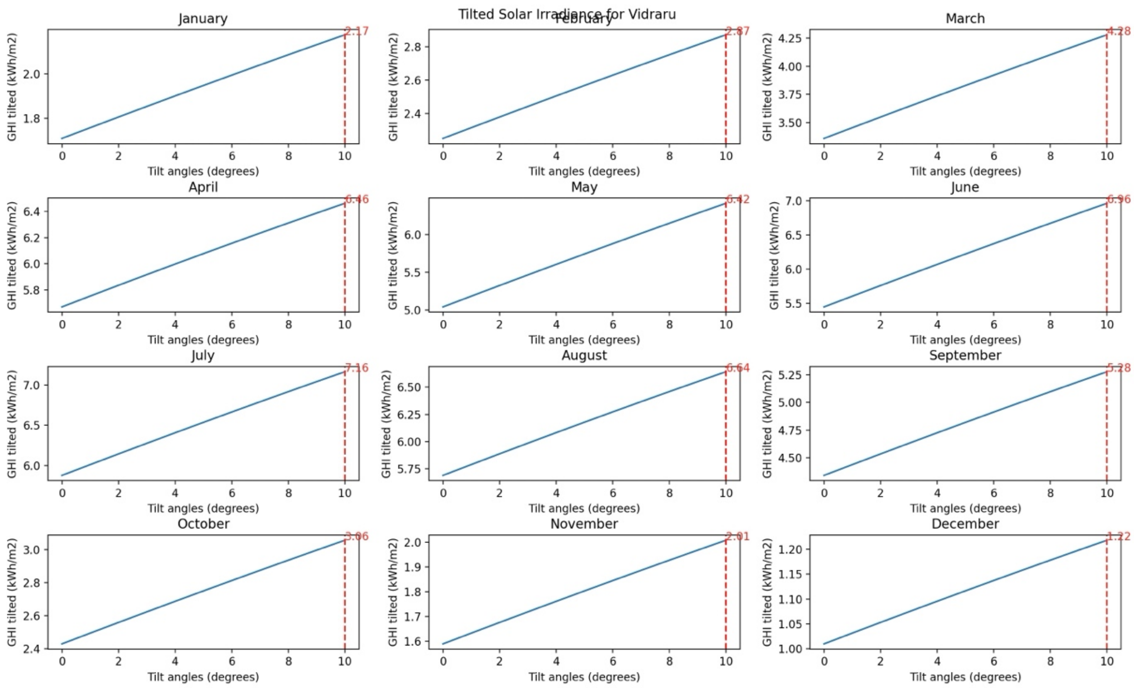

Fig. 4.27: Graphical monthly tilted GHI values for Lake Vidraru

4.9 (II) Analysis of the Optimal Locations for Solar Panels

In order to determine the optimal locations for installing solar panels, the same key criteria based on the statistical analysis of the solar irradiation must be taken into consideration (Table 4.20): the mean solar irradiation, the solar irradiation variability, and the minimum and maximum values, as described for Case I in Section 4.5.

Table 4.20: Centralised statistical values

Location	N	Mean kWh/m^2	Std. dev.	Min kWh/m^2	P25 kWh/m^2	Median (P50) kWh/m^2	P75 kWh/m^2	Max kWh/m^2	Range
Bicaz	12	4.55	2.27	0.88	2.79	4.86	6.36	7.61	6.73
Colibiţa	12	4.33	2.14	1.29	2.23	5.25	6.06	6.72	5.43
Goleşti	12	4.84	2.44	0.85	3.05	5.01	6.96	7.80	6.95
Oaşa	12	4.45	2.15	1.29	2.57	4.71	6.44	6.95	5.66
Vidra	12	4.45	2.15	1.28	2.57	4.71	6.44	6.96	5.68
Vidraru	12	4.60	2.16	1.22	2.70	4.78	6.51	7.16	5.94

The columns of the statistical table and the statistical equations used – the mean (equation (4.12)) and the standard deviation (equation (4.13)) – are the same as those described in detail for Case I in Section 4.5.1. The corresponding boxplot chart is presented in Figure 4.28.

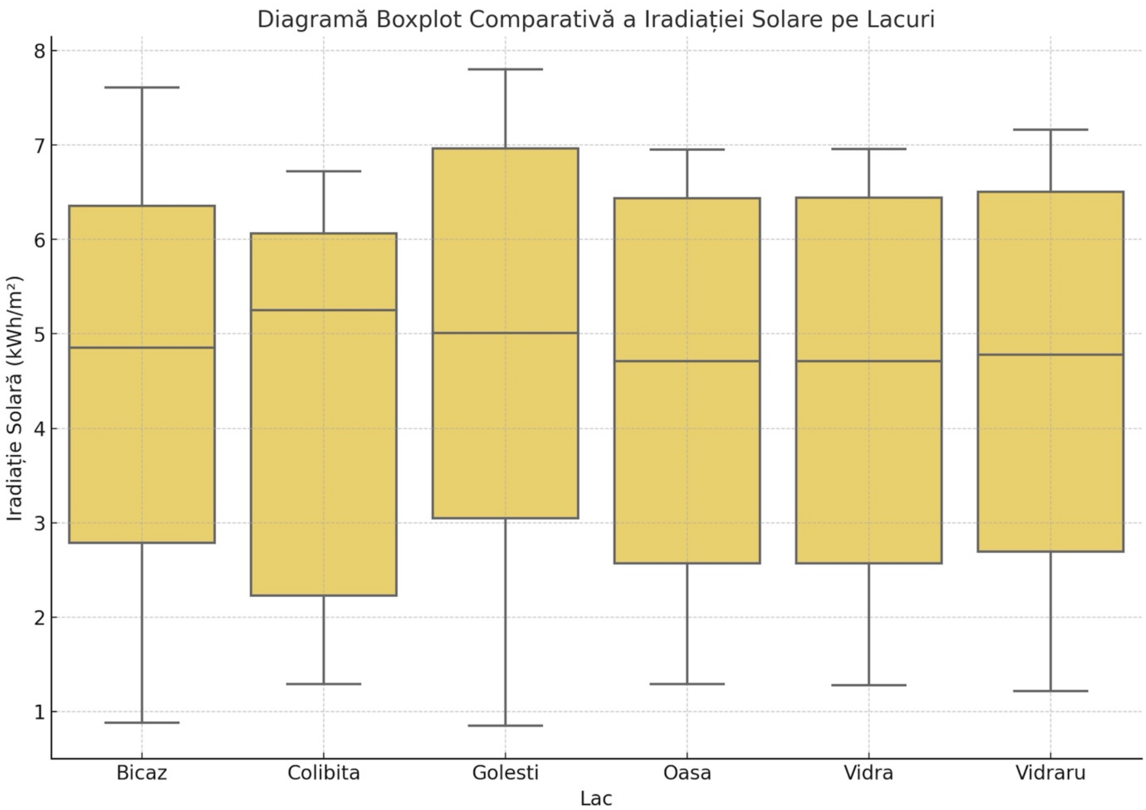

Fig. 4.28: Boxplot chart

4.10 (II) Description of the Statistical Chart: Boxplot of the Solar Irradiation

The boxplot chart presented illustrates the distribution of the solar irradiation values for each location included in the analysis at the 10-degree tilt angle. The elements of the boxplot chart (the box, the whiskers and the outliers) are the same as those described for Case I in Section 4.6.1.

4.10.1 (II) Observations from the chart

1. **Solar irradiation variability:**

  - *Wide ranges:* locations such as Bicaz and Goleşti show wide ranges of solar irradiation values, indicating significant variability throughout the year.
  - *Different medians:* the median solar irradiation varies between locations, showing differences in the mean level of solar energy received. For example, Goleşti has a higher median compared with Colibiţa.

2. **Extreme values (outliers):**
  - *Bicaz:* shows some high extreme values, suggesting periods with solar irradiation much higher than the mean.
  - *Colibiţa:* has fewer extreme values, which indicates a more uniform distribution of the solar irradiation.

3. **Comparison of the locations:**
  - *Bicaz:* has the highest solar irradiation variability, with a range from 0.88 kWh/m^2 to 7.61 kWh/m^2.
  - *Colibiţa:* has moderate variability, with a range from 1.29 kWh/m^2 to 6.72 kWh/m^2.
  - *Goleşti:* has a high median and consistently high values, which makes it favourable for solar energy projects, with a range from 0.85 kWh/m^2 to 7.80 kWh/m^2.
  - *Oaşa:* shows moderate variability, with a range from 1.29 kWh/m^2 to 6.95 kWh/m^2.
  - *Vidra:* has a variability similar to Oaşa, with a range from 1.28 kWh/m^2 to 6.96 kWh/m^2.
  - *Vidraru:* shows medium variability, with a range from 1.22 kWh/m^2 to 7.16 kWh/m^2.

Conclusions:

- **Solar project planning:** locations with higher means and smaller ranges are more predictable and can be more advantageous for solar energy projects. For example, Goleşti and Vidraru are promising locations owing to their high medians and moderate variability.
- **Risk analysis:** locations with high variability, such as Bicaz, might require additional risk management strategies, such as energy storage for periods of low irradiation.

4.11 (II) Optimal Locations for FPV Placement

4.11.1 (II) Lake Goleşti

- **Moderate mean:** 4.84 kWh/m^2.
- **High variability:** although the standard deviation and the range are relatively large, the maximum values are high, indicating a good potential for solar energy production. The range is from 0.85 kWh/m^2 to 7.80 kWh/m^2.

4.11.2 (II) Lake Vidraru

- **Moderate mean:** 4.60 kWh/m^2.
- **Moderate variability:** the minimum and maximum values are good, with a relatively large range, but with a high mean and constant production. The range is from 1.22 kWh/m^2 to 7.16 kWh/m^2.

4.11.3 (II) Lake Oaşa

- **Moderate mean:** 4.45 kWh/m^2.
- **Moderate variability:** the range and the standard deviation are moderate, providing a constant production. The range is from 1.29 kWh/m^2 to 6.95 kWh/m^2.

4.11.4 (II) Lake Bicaz

- **Moderate mean:** 4.55 kWh/m^2.
- **High variability:** shows the highest solar irradiation variability, with a range from 0.88 kWh/m^2 to 7.61 kWh/m^2.

4.11.5 (II) Lake Colibiţa

- **Moderate mean:** 4.33 kWh/m^2.
- **Moderate variability:** has a range from 1.29 kWh/m^2 to 6.72 kWh/m^2, indicating a more uniform distribution of the solar irradiation.

4.11.6 (II) Lake Vidra

- **Moderate mean:** 4.45 kWh/m^2.
- **Moderate variability:** the range is from 1.28 kWh/m^2 to 6.96 kWh/m^2, providing a constant production.

Conclusions (II):

- Goleşti and Vidraru are the suitable locations for installing solar panels owing to their high maximum values and moderate means, offering the potential for high electricity production.
- Oaşa, Bicaz, Colibiţa and Vidra have moderate means and acceptable variability, making them also good locations for solar energy production; however, the variability may require energy storage management during periods of low irradiation.
- Bicaz shows the highest variability, which may require additional energy storage solutions.

CHAPTER 5
CONCLUSIONS

The bachelor's thesis entitled "Floating Photovoltaic Panels: Assessing the Potential, Advantages and Challenges of Harvesting Solar Energy on Water Surfaces" explores an innovative and relevant topic in the context of the global transition towards renewable energy sources. The study provides a detailed analysis of floating photovoltaic panel (FPV) technology, evaluating its potential, advantages, disadvantages and environmental impact.

Chapter 1: Technology Overview

The first chapter presents the different types of floating platforms used for the installation of photovoltaic panels, such as buoyancy-based platforms, semi-submersible platforms and floating pontoons. The advantages and disadvantages of each type are discussed, highlighting the importance of corrosion-resistant materials and of designs adaptable to the conditions of the aquatic environment. The types of photovoltaic modules used are also detailed, such as second-generation CdTe, amorphous silicon (a-Si) and copper indium gallium selenide (CIGS), underlining their efficiency and adaptability in aquatic environments.

Chapter 2: Methods for Assessing the Potential of Floating Photovoltaic Panels

This chapter explores various tools and methods for assessing the energy potential of FPV. Platforms such as POWER, Solcast, PVsyst, PVGIS and SolarAtlas are analysed, which provide climate and solar data essential for the planning and development of renewable energy projects. These tools allow the simulation of photovoltaic system performance, the analysis of losses and yields, and the evaluation of the impact of weather conditions on energy production.

Chapter 3: Description of the Selected Sites

Chapter three provides a detailed description of the sites selected for FPV installation, such as the Izvorul Muntelui Hydropower Complex, Lake Vidraru and Lake Oaşa. The characteristics of each site are analysed, evaluating factors such as solar radiation, water conditions and site accessibility. This analysis allows the identification of the most suitable locations for FPV installation, thereby maximising energy efficiency and minimising the environmental impact.

Chapter 4: Assessment of the Solar Potential Using Geospatial Techniques

Chapter four provides a detailed analysis of the methodology and results obtained from the assessment of the energy potential of floating photovoltaic panels. The use of geospatial techniques and Python scripts for data processing enabled an efficient and accurate analysis. The simulation results indicate significant variations of the solar radiation depending on the season and identify the optimal locations for FPV placement.

1. **Study areas and methodology**

- *Selection of the study areas:* the reservoir lakes selected for the study, such as Lake Vidraru, Lake Oaşa and Lake Goleşti, were chosen on the basis of accessibility criteria, favourable weather conditions and the availability of geospatial data.
- *Computation methodology:* the use of Python scripts for data processing allowed an efficient and accurate analysis of the solar potential. The algorithm for the conversion of the global horizontal irradiance (GHI) into tilted GHI was essential for the correct estimation of the energy production.

2. **Simulation and computation results**

   - *GHI simulations:* the monthly values of the tilted global horizontal irradiance (GHI) were computed for each studied lake for two cases, with the panels tilted at 45 and 10 degrees respectively. These values indicated a significant variation of the solar radiation depending on the season, with maximum values in the summer months and minimum values in the winter months.
   - *Analysis of the optimal locations for both cases:* the data analysis identified the optimal locations for FPV placement. For example, Lake Goleşti and Lake Vidraru were identified as having a high solar potential owing to their consistent solar radiation levels and favourable environmental conditions, in both cases.

3. **Impact on water quality and the environment**

   - *Reduction of water evaporation:* FPV installations have demonstrated a significant positive impact in reducing water evaporation, thereby conserving water resources. It was found that FPV systems can reduce evaporation by up to 70%, contributing to the improvement of water quality and its conservation in water-scarce regions.
   - *Improvement of water quality:* studies have indicated that FPV installation can contribute to reducing algae growth and improving water quality. However, the impact varies depending on the water-surface coverage and the local specifics.

4. **Statistical analysis and visualisations**

   - *Statistical charts:* boxplots and other graphical representations were used to visualise the distribution of the solar radiation and the performance of FPV systems at the studied locations. These charts provided a clear picture of the solar radiation variability and helped identify trends and anomalies.
   - *Statistical data:* the collected statistical data were used to evaluate the potential performance of FPV under different climatic conditions. The results showed that the studied locations can provide a consistent solar energy production with minimal variability throughout the year.

Final Results and Conclusions

The results obtained from the studies and simulations presented in this work indicate that floating photovoltaic panels represent a viable and efficient solution for solar energy generation, especially in areas with limited land resources. The main advantages of FPV include:

- **High energy efficiency:** FPV systems can have an efficiency of up to 12.5% higher compared with land-based photovoltaic systems owing to the cooling effect of the water.

- **Reduction of water evaporation:** FPV contributes to reducing water evaporation from reservoirs, conserving water resources and improving water quality.
- **Minimisation of the environmental impact:** by using water surfaces for the installation of solar panels, land-use conflicts and the negative impact on terrestrial ecosystems are reduced.
- **Economic potential:** FPV offers an economical solution in regions where land is expensive or unavailable, reducing acquisition and installation costs.

The thesis underlines the importance of continuing research in the FPV field in order to optimise the design and performance of these systems, while ensuring environmental protection and the sustainability of natural resources. The large-scale implementation of floating photovoltaic panels can play a crucial role in achieving the global goals of reducing greenhouse gas emissions and transitioning towards a sustainable energy future.

BIBLIOGRAPHY

[1] *Abbasnia, A., et al.* (2022). Wind parameters effects on floating solar array design – case study: Japan's largest floating solar array. In: Proc. of the International Conference on Offshore Mechanics and Arctic Engineering – OMAE 8. https://doi.org/10.1115/OMAE2022-78762

[2] *Abdelal, Q.* (2021). Floating PV; an assessment of water quality and evaporation reduction in semi-arid regions. International Journal of Low-Carbon Technologies, 16(3), 732–739. https://doi.org/10.1093/IJLCT/CTAB001

[3] *Abdurohman, K., Adhitya, M.* (2019). Effect of water and seawater on mechanical properties of fiber reinforced polymer composites: a review for amphibious aircraft float development. IOP Conference Series: Materials Science and Engineering, 694(1), 012035. https://doi.org/10.1088/1757-899X/694/1/012035

[4] *Abid, M., et al.* (2019). Prospects of floating photovoltaic technology and its implementation in Central and South Asian Countries. International Journal of Environmental Science and Technology, 16(3), 1755–1762. https://doi.org/10.1007/S13762-018-2080-5

[5] *Al-Widyan, M., Khasawneh, M., Abu-Dalo, M.* (2021). Potential of floating photovoltaic technology and their effects on energy output, water quality, and supply in Jordan. Energies, 14(24), 8417. https://doi.org/10.3390/EN14248417

[6] *Azni, M.A., et al.* (2023). Review of the effects of fossil fuels and the need for a hydrogen fuel cell policy in Malaysia. Sustainability, 15(5), 4033. https://doi.org/10.3390/SU15054033

[7] *Banik, A., Sengupta, A.* (2021). Scope, challenges, opportunities, and future goal assessment of floating solar park. Innovations in Energy Management and Renewable Resources, IEMRE 2021. https://doi.org/10.1109/IEMRE52042.2021.9386735

[8] *Cazzaniga, R., et al.* (2019). Integration of PV floating with hydroelectric power plants. Heliyon. https://doi.org/10.1016/j.heliyon.2019.e01918

[9] *Cazzaniga, R.* (2020). Floating PV Structures. Floating PV Plants, 33–45. https://doi.org/10.1016/B978-0-12-817061-8.00004-X

[10] *Cazzaniga, R., Rosa-Clot, M.* (2021). The booming of floating PV. Solar Energy, 219, 3–10. https://doi.org/10.1016/J.SOLENER.2020.09.057

[11] *Claus, R., López, M.* (2022). Key issues in the design of floating photovoltaic structures for the marine environment. Renewable and Sustainable Energy Reviews, 164, 112502. https://doi.org/10.1016/J.RSER.2022.112502

[12] *Cuce, E., et al.* (2022). Floating PVs in Terms of Power Generation, Environmental Aspects, Market Potential, and Challenges. Sustainability, 14(5), 2626. https://doi.org/10.3390/SU14052626

[13] *Donaghy, T.Q., et al.* (2023). Fossil fuel racism in the United States: How phasing out coal, oil, and gas can protect communities. Energy Research & Social Science, 100, 103104. https://doi.org/10.1016/J.ERSS.2023.103104

[14] *Dwivedi, P., et al.* (2020). Advanced cooling techniques of P.V. modules: A state of art. Case Studies in Thermal Engineering, 21, 100674. https://doi.org/10.1016/J.CSITE.2020.100674

[15] *Edwards, E.C., et al.* (2023). Evolution of floating offshore wind platforms: A review of at-sea devices. Renewable and Sustainable Energy Reviews, 183, 113416. https://doi.org/10.1016/J.RSER.2023.113416

[16] *Enaganti, P.K., et al.* (2022). Experimental investigations for dust build-up on low-iron glass exterior and its effects on the performance of solar PV systems. Energy, 239, 122213. https://doi.org/10.1016/J.ENERGY.2021.122213

[17] *Essak, L., Ghosh, A.* (2022). Floating Photovoltaics: A Review. Clean Technologies, 4(3), 752–769. https://doi.org/10.3390/CLEANTECHNOL4030046

[18] *Exley, G., et al.* (2021a). Floating photovoltaics could mitigate climate change impacts on water body temperature and stratification. Solar Energy, 219, 24–33. https://doi.org/10.1016/J.SOLENER.2021.01.076

[19] *Exley, G., et al.* (2021b). Scientific and stakeholder evidence-based assessment: Ecosystem response to floating solar photovoltaics and implications for sustainability. Renewable and Sustainable Energy Reviews, 152, 111639. https://doi.org/10.1016/J.RSER.2021.111639

[20] *Farrar, L.W., et al.* (2022). Floating solar PV to reduce water evaporation in water-stressed regions and powering water pumping: Case study Jordan. Energy Conversion and Management, 260, 115598. https://doi.org/10.1016/J.ENCONMAN.2022.115598

[21] *Fereshtehpour, M., et al.* (2021). Evaluation of factors governing the use of floating solar system: A study on Iran's important water infrastructures. Renewable Energy, 171, 1171–1187. https://doi.org/10.1016/J.RENENE.2020.12.005

[22] *Gadzanku, S., et al.* (2021a). Benefits and Critical Knowledge Gaps in Determining the Role of Floating Photovoltaics in the Energy-Water-Food Nexus. Sustainability, 13(8), 4317. https://doi.org/10.3390/SU13084317

[23] *Gadzanku, S., Beshilas, L., Grunwald, U.* (2021b). Enabling Floating Solar Photovoltaic (FPV) Deployment: Review of Barriers to FPV Deployment in Southeast Asia. https://doi.org/10.2172/1787553

[24] *Ghosh, A.* (2023). A comprehensive review of water based PV: Flotavoltaics under water, offshore & canal top. Ocean Engineering, 281, 115044. https://doi.org/10.1016/J.OCEANENG.2023.115044

[25] *Goswami, A., et al.* (2019). Floating solar power plant for sustainable development: A techno-economic analysis. Environmental Progress & Sustainable Energy, 38(6), e13268. https://doi.org/10.1002/EP.13268

[26] *Grant, N.E., et al.* (2020). Lifetime instabilities in gallium doped monocrystalline PERC silicon solar cells. Solar Energy Materials and Solar Cells, 206, 110299. https://doi.org/10.1016/J.SOLMAT.2019.110299

[27] *Haas, J., et al.* (2020). Floating photovoltaic plants: Ecological impacts versus hydropower operation flexibility. Energy Conversion and Management, 206, 112414. https://doi.org/10.1016/J.ENCONMAN.2019.112414

[28] *Jiang, Z., et al.* (2023). Design and model test of a soft-connected lattice-structured floating solar photovoltaic concept for harsh offshore conditions. Marine Structures, 90, 103426. https://doi.org/10.1016/J.MARSTRUC.2023.103426

[29] *Jin, Y., et al.* (2023). Energy production and water savings from floating solar photovoltaics on global reservoirs. Nature Sustainability, 6(7), 865–874. https://doi.org/10.1038/s41893-023-01089-6

[30] *Kaliyannan, G.V., et al.* (2023). Thin-Film Solar Cells. Fundamentals of Solar Cell Design, 103–115. https://doi.org/10.1002/9781119725022.CH4

[31] *Kaplanis, S., Kaplani, E., Kaldellis, J.K.* (2023). PV Temperature Prediction Incorporating the Effect of Humidity and Cooling Due to Seawater Flow and Evaporation on Modules Simulating Floating PV Conditions. Energies, 16(12), 4756. https://doi.org/10.3390/EN16124756

[32] *Kaymak, M.K., Şahin, A.D.* (2021). Problems encountered with floating photovoltaic systems under real conditions: A new FPV concept and novel solutions. Sustainable Energy Technologies and Assessments, 47, 101504. https://doi.org/10.1016/J.SETA.2021.101504

[33] *Kazem, H.A., et al.* (2020). A review of dust accumulation and cleaning methods for solar photovoltaic systems. Journal of Cleaner Production, 276, 123187. https://doi.org/10.1016/J.JCLEPRO.2020.123187

[34] *Kumar, M., Mohammed, N.H., Gupta, R.* (2021). Challenges and opportunities towards the development of floating photovoltaic systems. Solar Energy Materials and Solar Cells, 233, 111408. https://doi.org/10.1016/J.SOLMAT.2021.111408

[35] *Lee, N., et al.* (2020). Hybrid floating solar photovoltaics-hydropower systems: Benefits and global assessment of technical potential. Renewable Energy, 162, 1415–1427. https://doi.org/10.1016/J.RENENE.2020.08.080

[36] *Li, M., et al.* (2022). State-of-the-art review of the flexibility and feasibility of emerging offshore and coastal ocean energy technologies in East and Southeast Asia. Renewable and Sustainable Energy Reviews, 162, 112404. https://doi.org/10.1016/J.RSER.2022.112404

[37] *Liang, Y., Kleijn, R., van der Voet, E.* (2023). Increase in demand for critical materials under IEA Net-Zero emission by 2050 scenario. Applied Energy, 346, 121400. https://doi.org/10.1016/J.APENERGY.2023.121400

[38] *Lima, M.A., et al.* (2020). Renewable energy in reducing greenhouse gas emissions: Reaching the goals of the Paris agreement in Brazil. Environmental Development, 33, 100504. https://doi.org/10.1016/J.ENVDEV.2020.100504

[39] *Luo, W., et al.* (2021). Performance loss rates of floating photovoltaic installations in the tropics. Solar Energy, 219, 58–64. https://doi.org/10.1016/J.SOLENER.2020.12.019

[40] *Makahleh, F.M., et al.* (2023). Optimal Management of Energy Storage Systems for Peak Shaving in a Smart Grid. Computers, Materials & Continua, 75(2), 3317–3337. https://doi.org/10.32604/CMC.2023.035690

[41] *Mayville, P., Patil, N.V., Pearce, J.M.* (2020). Distributed manufacturing of after-market flexible floating photovoltaic modules. Sustainable Energy Technologies and Assessments, 42, 100830. https://doi.org/10.1016/J.SETA.2020.100830

[42] *Micheli, L.* (2022). The temperature of floating photovoltaics: Case studies, models and recent findings. Solar Energy, 242, 234–245. https://doi.org/10.1016/J.SOLENER.2022.06.039

[43] *Muhammad, S., et al.* (2023). Application of Dynamic Programming for Optimal Hybrid Energy Management System: Hydro-Photovoltaic-Diesel-BESS. IEEE Access. https://doi.org/10.1109/ACCESS.2023.3296699

[44] *Muñoz-Cerón, E., et al.* (2023). Floating photovoltaics systems on water irrigation ponds: Technical potential and multi-benefits analysis. Energy, 271, 127039. https://doi.org/10.1016/J.ENERGY.2023.127039

[45] *Nagananthini, R., Nagavinothini, R.* (2021). Investigation on floating photovoltaic covering system in rural Indian reservoir to minimize evaporation loss. International Journal of Sustainable Energy, 40(8), 781–805. https://doi.org/10.1080/14786451.2020.1870975

[46] *Natarajan, S.K., et al.* (2019). Design and development of dual axis sun tracking system for floating PV plant. IOP Conference Series: Earth and Environmental Science, 312(1), 012001. https://doi.org/10.1088/1755-1315/312/1/012001

[47] *Ndumnu, N., et al.* (n.d.). Floating PV Technology and its Possible Applications. https://www.researchgate.net/publication/344714482 (Accessed: 27 July 2023)

[48] *Nisar, H., et al.* (2022). Thermal and electrical performance of solar floating PV system compared to on-ground PV system – an experimental investigation. Solar Energy, 241, 231–247. https://doi.org/10.1016/J.SOLENER.2022.05.062

[49] *Patil, A., Mamatha, G., Kulkarni, P.S.* (2022). Techno-Economic Analysis of proposed 10 kWp Floating Solar Plant at Koyana Dam, Maharashtra, India. In: Proc. of the 2nd International Conference on Power Electronics and IoT Applications in Renewable Energy and its Control, PARC 2022. https://doi.org/10.1109/PARC52418.2022.9726247

[50] *Piana, V., et al.* (2021). Floating PV in mountain artificial lakes: a checklist for site assessment. Renewable Energy and Environmental Sustainability, 6, 4. https://doi.org/10.1051/REES/2021002

[51] *Qureshi, O.A., et al.* (2023). Thermal or photovoltaic rear sides? A parametric comparison between photovoltaic thermal and bifacial technology. Energy Conversion and Management, 289, 117134. https://doi.org/10.1016/J.ENCONMAN.2023.117134

[52] *Rauf, A., et al.* (2023). The current developments and future prospects of solar photovoltaic industry in an emerging economy of India. Environmental Science and Pollution Research, 30(16), 46270–46281. https://doi.org/10.1007/S11356-023-25471-1

[53] *Refaai, M.R.A., et al.* (2022). Design and Implementation of a Floating PV Model to Analyse the Power Generation. International Journal of Photoenergy, 2022. https://doi.org/10.1155/2022/3891881

[54] *Rosa-Clot, M., Tina, G.M.* (2020). Current Status of FPV and Trends. Floating PV Plants, 9–18. https://doi.org/10.1016/B978-0-12-817061-8.00002-6

[55] *Rosa-Clot, P.* (2020). FPV and Environmental Compatibility. Floating PV Plants, 101–118. https://doi.org/10.1016/B978-0-12-817061-8.00009-9

[56] *Schreier, S., et al.* (2022). Committee V.6: Ocean Space Utilization. In: Proc. of the 21st International Ship and Offshore Structures Congress, ISSC 2022, 2, 379–444. https://doi.org/10.5957/ISSC-2022-COMMITTEE-V-6

[57] *Solar Energy Research Institute of Singapore* (2018). Where Sun Meets Water: Floating Solar Market Report. Washington.

[58] *Solomin, E., et al.* (2021). Hybrid floating solar plant designs: A review. Energies, 14(10), 2751. https://doi.org/10.3390/EN14102751

[59] *Vartiainen, E., et al.* (2020). Impact of weighted average cost of capital, capital expenditure, and other parameters on future utility-scale PV levelised cost of electricity. Progress in Photovoltaics: Research and Applications, 28(6), 439–453. https://doi.org/10.1002/PIP.3189

[60] *Vidović, V., et al.* (2023). Review of the potentials for implementation of floating solar panels on lakes and water reservoirs. Renewable and Sustainable Energy Reviews, 178, 113237. https://doi.org/10.1016/J.RSER.2023.113237

[61] *Vo, T.T.E., et al.* (2021). Overview of possibilities of solar floating photovoltaic systems in the offshore industry. Energies, 14(21), 6988. https://doi.org/10.3390/EN14216988

[62] *Wijewardane, S., Kazmerski, L.L.* (2023). Inventions, innovations, and new technologies: Flexible and lightweight thin-film solar PV based on CIGS, CdTe, and a-Si:H. Solar Compass, 7, 100053. https://doi.org/10.1016/J.SOLCOM.2023.100053

[63] *Yang, P., et al.* (2022). Impacts of a floating photovoltaic system on temperature and water quality in a shallow tropical reservoir. Limnology, 23(3), 441–454. https://doi.org/10.1007/S10201-022-00698-Y

[64] *Piştoia, I., Buta, I.* Hidrologie.

[65] *Romanian National Committee on Large Dams*. Dams in Romania.

ANNEX 1. PYTHON SCRIPT FOR EXTRACTING AND PROCESSING THE DAILY DNI AND GHI DATA

```
import requests
import pandas as pd
from datetime import datetime

latitude = "45.375287"
longitude = "24.62936"
tilt = 18  # Constant value for the tilt

params = {
    "parameters": "ALLSKY_SFC_SW_DWN,ALLSKY_SFC_SW_DNI",
    "community": "RE",
    "longitude": longitude,
    "latitude": latitude,
    "format": "JSON",
    "start": "20200101",
    "end": "20201231",
    "tempAverage": "DAILY",
    "time": "24"
}

url = "https://power.larc.nasa.gov/api/temporal/daily/point"
response = requests.get(url, params=params)

if response.status_code == 200:
    data = response.json()
    records = []
    ghi_data = data['properties']['parameter']['ALLSKY_SFC_SW_DWN']
    dni_data = data['properties']['parameter']['ALLSKY_SFC_SW_DNI']
    for date_str in ghi_data:
        readable_date = datetime.strptime(date_str, "%Y%m%d")
        dni_value = dni_data.get(date_str, 'N/A')
        records.append({
            'Date': readable_date,
            'Longitude': longitude,
            'Latitude': latitude,
            'Tilt': tilt,
            'DNI': dni_value,
            'GHI': ghi_data[date_str]
        })
    df = pd.DataFrame(records)
    df['Date'] = pd.to_datetime(df['Date'])
```

```
    df['YearMonth'] = df['Date'].dt.to_period('M')
    monthly_avg = df.groupby('YearMonth').agg(
        {'DNI': 'mean', 'GHI': 'mean'}).reset_index()
    monthly_days = df.groupby('YearMonth').size().reset_index(name='Days')
    monthly_data = pd.merge(monthly_avg, monthly_days, on='YearMonth')
    # Round the DNI and GHI values to 2 decimals
    monthly_data['DNI'] = monthly_data['DNI'].round(2)
    monthly_data['GHI'] = monthly_data['GHI'].round(2)
    monthly_data['Longitude'] = float(longitude)
    monthly_data['Latitude'] = float(latitude)
    monthly_data['Tilt'] = tilt
    monthly_data = monthly_data[['Days', 'Longitude', 'Latitude',
                                 'Tilt', 'DNI', 'GHI']]
    # Name of the CSV file where the monthly data will be saved
    csv_file_path = '.../ImportDniGhi/Vidraru.csv'
    # Saving the computed data to a new CSV file
    monthly_data.to_csv(csv_file_path, index=False)
    print(f"The monthly data have been computed and saved to "
          f"'{csv_file_path}'")
else:
    print("Error downloading the data: ", response.status_code)
```

ANNEX 2. COMPUTATION OF THE GLOBAL HORIZONTAL IRRADIANCE ON TILTED SURFACES

```
import math
import matplotlib.pyplot as plt
import pandas as pd
import csv
import os

pi = math.pi

def deg_to_rad(theta):
    return theta * (2 * pi) / 360

def rad_to_rad(theta):
    return theta * 360 / (2 * pi)

def load_data(filenames):
    data_frames = {}
    for lake, file in filenames.items():
        data_frames[lake] = pd.read_csv(file)
    return data_frames

lake_files = {
    'Colibita': '.../Proiect Adaptat Licenta/Colibita.csv',
    'Vidra': '.../Proiect Adaptat Licenta/Vidra.csv',
    'Golesti': '.../Proiect Adaptat Licenta/Golesti.csv',
    'Oasa': '.../Proiect Adaptat Licenta/Oasa.csv',
    'Vidraru': '.../Proiect Adaptat Licenta/Vidraru.csv',
    'Bicaz': '.../Proiect Adaptat Licenta/Bicaz.csv',
}

data_frames = load_data(lake_files)

hsc = 1.353  # Solar constant value

def calculate_irradiance(df):
    results = []
    for index, row in df.iterrows():
        n = row['Days']
        latitude = row['Latitude']
        longitude = row['Longitude']
        tilt = row['Tilt']
        dni = row['DNI']
```

```
        ghi = row['GHI']
        delta = 23.45 * math.sin(deg_to_rad(360 * (284 + n) / 365))
        rb = (math.sin(deg_to_rad(latitude - tilt)) *
              math.sin(deg_to_rad(delta)) +
              math.cos(deg_to_rad(latitude - tilt)) *
              math.cos(deg_to_rad(delta)) *
              math.cos(deg_to_rad(longitude))) / (
             math.sin(deg_to_rad(latitude)) *
             math.sin(deg_to_rad(delta)) +
             math.cos(deg_to_rad(latitude)) *
             math.cos(deg_to_rad(longitude)) *
             math.cos(deg_to_rad(delta)))
        rd = (1 + math.cos(deg_to_rad(tilt))) / 2
        rr = (1 - math.cos(deg_to_rad(tilt))) / 2
        hs = rad_to_rad(math.acos(-math.tan(deg_to_rad(latitude)) *
                                  math.tan(deg_to_rad(delta))))
        ho = ((hsc / pi) * 24) * (1 + 0.033 *
              math.cos(deg_to_rad(360 * n) / 365)) * (
             (math.cos(deg_to_rad(latitude)) *
              math.cos(deg_to_rad(delta)) *
              math.sin(deg_to_rad(hs))) +
             ((((2 * pi) / 360) * hs) *
              math.sin(deg_to_rad(latitude)) *
              math.sin(deg_to_rad(delta))))
        kt = dni / ho
        hd = ghi * ((0.775 + (0.00653 * (hs - 90))) -
                    (0.505 + (0.00455 * (hs - 90))) *
                    (math.cos(deg_to_rad(115 * kt - 103))))
        hb = (ghi - hd)
        roh = 0.5
        hr = ghi * roh
        ht = hr * rr + hb * rb + hd * rd
        results.append(ht)
    return results

months = ['January', 'February', 'March', 'April', 'May', 'June',
          'July', 'August', 'September', 'October', 'November',
          'December']

def calculate_monthly_irradiance(lake_name, df):
    monthly_irradiance = {month: [] for month in months}
    for tilt_angle in range(0, 11):  # Tilt angles 0 to 10 degrees
        df['Tilt'] = tilt_angle
        irradiance = calculate_irradiance(df)
        for i, month in enumerate(months):
            monthly_irradiance[month].append(irradiance[i])
    return monthly_irradiance

def find_max_irradiance(monthly_irradiance):
    max_irradiance = {}
    for month in months:
        max_value = max(monthly_irradiance[month])
        max_angle = monthly_irradiance[month].index(max_value)
        max_irradiance[month] = (max_angle, max_value)
    return max_irradiance

def plot_irradiance(lake_name, monthly_irradiance, max_irradiance):
```

```
    plt.figure(figsize=(15, 10))
    for i, month in enumerate(months):
        plt.subplot(4, 3, i + 1)
        plt.plot(range(0, 11), monthly_irradiance[month])
        plt.xlabel('Tilt angles (degrees)')
        plt.ylabel('GHI tilted (kWh/m2)')
        plt.title(f'{month}')
        max_angle, max_value = max_irradiance[month]
        plt.axvline(x=max_angle, color='r', linestyle='--')
        plt.text(max_angle, max_value, f'{max_value:.2f}', color='red')
    plt.tight_layout()
    plt.suptitle(f'Tilted Solar Irradiance for {lake_name}')
    plt.subplots_adjust(top=0.95)
    plt.show()

def analyze_lake(lake_name):
    df = data_frames[lake_name]
    monthly_irradiance = calculate_monthly_irradiance(lake_name, df)
    max_irradiance = find_max_irradiance(monthly_irradiance)
    plot_irradiance(lake_name, monthly_irradiance, max_irradiance)
    results = []
    for month in months:
        angle, value = max_irradiance[month]
        results.append([lake_name, month, angle, round(value, 2)])
        print(f'The maximum value of tilted solar irradiance on the '
              f'{lake_name} for the month {month} happens at a tilt '
              f'angle {angle} degrees and the corresponding solar '
              f'irradiance is {round(value, 2)}')
    csv_file = f'.../{lake_name}_solar_irradiance.csv'
    with open(csv_file, mode='w', newline='') as file:
        writer = csv.writer(file)
        writer.writerow(['Lake', 'Month', 'Tilt Angle (degrees)',
                         'Solar Irradiance (kWh/m2)'])
        writer.writerows(results)
    print(f'Results have been saved to {csv_file}')

analyze_lake('Vidraru')
```